

C.P. No.635

LIBRARY  
ROYAL AIRCRAFT ESTABLISHMENT  
BEDFORD.

C.P. No.635



MINISTRY OF AVIATION

AERONAUTICAL RESEARCH COUNCIL

CURRENT PAPERS

# Three-Dimensional Turbulent Boundary Layers

by

*J. C. Cooke, D.Sc.*

LONDON: HER MAJESTY'S STATIONERY OFFICE

1963

PRICE 8s 6d NET

U.D.C. No. 532.526.4 : 532.517.4 : 532.517.3

C.P. No. 635

June, 1961

THREE-DIMENSIONAL TURBULENT BOUNDARY LAYERS

by

J. C. Cooke, D.Sc.

---

SUMMARY

This paper reviews the current state of knowledge of three-dimensional turbulent boundary layers, mainly from the point of view of making calculations. The nature of the boundary layer is discussed and the equations for general steady turbulent flow are given. Next follow momentum-integral equations, which can then be solved with suitable assumptions as to the velocity profiles and shear stress components. An account of these assumptions follows and a few sample results are given. The paper ends with a short account of some matters connected with transition.

## LIST OF CONTENTS

	<u>Page</u>
1 INTRODUCTION	4
2 GENERAL	5
2.1 Boundary layer and momentum-integral equations	5
2.2 Three-dimensional effects	8
2.3 The axially symmetric analogy	9
3 VELOCITY PROFILES AND SKIN FRICTION COMPONENTS	11
3.1 Velocity profiles	12
3.2 Wall friction values	16
4 GENERAL METHODS	17
4.1 Cooke's method	18
4.2 Becker's method	19
4.3 Johnston's solution along a line of symmetry	22
4.4 Braun's solution for the slightly yawed cone	24
5 TRANSITION	24
6 CONCLUDING REMARKS	25
LIST OF SYMBOLS	26
LIST OF REFERENCES	28
ILLUSTRATIONS - Figs 1-17	-
DETACHABLE ABSTRACT CARDS	-

## LIST OF ILLUSTRATIONS

	<u>Fig.</u>
Laminar cross-flow velocity profiles. External point of inflexion at $\xi = 0.5$	1
Oil flow patterns showing wedges of turbulence (Brebner and Wyatt)	2
Experimental arrangement of Johnston	3
Johnston's form for the cross-flow	4
Polar plots by Johnston from data of Kuethe, McKee and Curry	5
Cross-flow according to Johnston's model with $u/u_e = (\zeta/\delta)^{1/7}$ , $e = 1.47$ , $A = 0.26$	6
Isometric figure for the velocity distributions of Fig.6	7

LIST OF ILLUSTRATIONS (Cont'd)

	<u>Fig.</u>
Wake components $w_h$ and $w_j$ . (Blackman and Joubert)	8
Values of $\theta_{11}$ and $\delta_1$ from measurements by Brebner and Wyatt	9
Values of $\alpha$ for measurements by Brebner and Wyatt	10
Calculated external streamlines on delta wing at zero incidence (Cooke)	11
Growth of momentum thickness along streamlines of Fig.11 (Cooke)	12
Deflection of limiting streamlines on yawed cone (Braun)	13
Possible transition front (Cooke)	14
Development of upper surface showing calculated streamline at $-3^\circ$ incidence and calculated shapes of turbulent wedges for $x/c = 0.20, 0.05, 0.02$ and $0.01$ positions (Gregory)	15
Spread of turbulence due to conical excrescences on $60^\circ$ swept wing. From photographs by Gregory	16
Momentum and displacement thicknesses at transition. From curves drawn by Rotta from measurements on a flat plate by Schubauer and Klebanoff	17

The study of three-dimensional turbulent boundary layers has been greatly neglected in the literature. Thus in two reviews, one by Sears<sup>1</sup> in 1954 and one by Moore<sup>2</sup> in 1956 which together include about 50 references on the subject of three-dimensional boundary layers, only 4 refer to the turbulent problem and these were all concerned with flow over infinite yawed wings and cannot be considered to be quite general. In the review by Cooke and Hall<sup>3</sup>, written in 1960, there are about 50 more references, and of these only about 12 refer to genuinely three-dimensional turbulent boundary layers. Again, in Applied Mechanics Reviews for 1960 there are about 175 references to boundary layers of all kinds (excluding Magnetohydrodynamics) of which only 1 deals with a properly three-dimensional turbulent problem, whilst two others do so in part (and only a small part). Since flying machines of the future are likely to be more "three-dimensional" in shape than in the past it will certainly be necessary to make a greater study of the subject than has been done up to the present time. The neglect has been due to the difficulties of the subject, which are immense, even in two dimensions, and to the fact that the collecting of experimental evidence is so tedious and unrewarding.

This paper is an attempt to review what little that has been done. In it we shall exclude unsteady mean flows and will also exclude in the main axially symmetric flow, since the latter has usually merely involved a simple extension to work on two-dimensional flow. Attention will be concentrated almost entirely on theoretical work, and in particular on the description of such calculation methods as have been attempted. These have all assumed small (or zero) cross-flow, that is, small mean velocity components normal to the streamlines in the external flow, and have assumed well-known two-dimensional expressions for the streamwise velocity and skin friction components. More variety has been found in the assumptions for the cross-flow. The only more unified attempt to write down a general form for the velocity profiles is due to Coles<sup>4</sup>. This is an extension of the law of the wall and the law of the wake; so far only a small amount of experimental evidence exists in support of this model. The subject has been deeply examined by Johnston<sup>5,6</sup> who suggested a form for the cross-flow quite different from any of the others and presented considerable experimental evidence in its support.

The flow over infinite yawed wings has considerable literature in laminar flow. This is because there exists an "independence" principle according to which the chordwise components of flow satisfy ordinary two-dimensional boundary layer equations. This principle does not hold for turbulent flow. A simple theoretical proof of this was given by Rott and Crabtree<sup>7</sup> and experiments of Ashkenas and Riddell<sup>8</sup> confirmed it. A full discussion of the subject was given by Turcotte<sup>9</sup>, who advocated a "line of flow" principle, by which the streamwise wall shear stress is considered to be a function of the distance over which the fluid has actually flowed, rather than the perpendicular distance from the leading edge. Most methods of calculation so far put forward have used streamline co-ordinates and they have tacitly followed this principle.

Turbulent separation in three-dimensions has scarcely been touched upon by workers in the field, except in its purely topological aspects, which apply equally well to laminar or turbulent boundary layers<sup>10,11</sup>. We do not consider it here.

In this paper we give the general three-dimensional equations for the mean flow, and then explain the axially symmetric analogy applicable in cases where the mean cross-flow is small. Momentum-integral equations are given, since only by their use has any progress been made. Their solution depends on assumptions made about velocity profiles and surface shear stress.

An account of these assumptions follows. Next is given a description of the few three-dimensional turbulent boundary layer calculations that have been made, and we conclude with a short account of some matters connected with transition.

## 2 GENERAL

### 2.1 Boundary layer and momentum-integral equations

Curvilinear co-ordinates  $\xi, \eta, \zeta$  are used. The surface over which the boundary layer lies is  $\zeta = 0$  and  $\zeta$  denotes distance from the surface measured along a normal. On the surface  $\zeta = 0$  are two families of co-ordinate curves  $\xi = \text{constant}$  and  $\eta = \text{constant}$ , orthogonal to one another. For this system the element of length is given by

$$ds^2 = h_1^2 d\xi^2 + h_2^2 d\eta^2 + d\zeta^2. \quad (1)$$

In the boundary layer  $h_1$  and  $h_2$  are usually assumed to be functions of  $\xi$  and  $\eta$  only. For this to hold it is necessary that the curvature of the surface does not change abruptly and that locally the boundary layer thickness is small compared to the principal radii of curvature of the surface.

We denote velocity components by  $u + u', v + v', w + w'$ , where  $u, v$  and  $w$  are the mean values. Density  $\rho$ , total enthalpy  $\bar{H}$  and temperature  $T$  are treated in the same way. Terms involving fluctuations of the coefficient of viscosity  $\mu$ , the coefficient of heat conductivity, the specific heat at constant pressure  $c_p$  and the Prandtl number  $Pr$  are omitted. Mean squares and products of the turbulent fluctuations in velocity and density are taken to be of order  $\delta$ , the boundary layer thickness. As in the incompressible two-dimensional case this last assumption is probably justified in favourable or slightly unfavourable pressure gradients, but is not so when separation is approached. The usual boundary layer approximation, namely that rates of change of mean flow properties in the  $\xi$  and  $\eta$  directions are of order unity and those in the  $\zeta$  direction are of order  $\delta^{-1}$ , are made. We write

$$K_1 = -\frac{1}{h_1 h_2} \frac{\partial h_2}{\partial \xi}, \quad K_2 = -\frac{1}{h_1 h_2} \frac{\partial h_1}{\partial \eta}; \quad (2)$$

these are the geodesic curvatures of the curves  $\xi = \text{constant}$ ,  $\eta = \text{constant}$  respectively. We denote the mean of a product  $f'g'$  by  $\overline{f'g'}$ . A full account of the derivation of the equations of motion is given by Vaglio-Laurin<sup>12</sup>. For steady mean flow, in the absence of body forces and of heat sources the equations are

$$\begin{aligned} \frac{u}{h_1} \frac{\partial u}{\partial \xi} + \frac{v}{h_2} \frac{\partial u}{\partial \eta} + \left[ w + \frac{\overline{(\rho'w')}}{\rho} \right] \frac{\partial u}{\partial \zeta} - K_2 uv + K_1 v^2 \\ = -\frac{1}{\rho h_1} \frac{\partial p}{\partial \xi} + \frac{1}{\rho} \frac{\partial}{\partial \zeta} \left[ \mu \frac{\partial u}{\partial \zeta} - \rho \overline{(u'w')} \right], \end{aligned} \quad (3)$$

$$\begin{aligned} \frac{u}{h_1} \frac{\partial v}{\partial \xi} + \frac{v}{h_2} \frac{\partial v}{\partial \eta} + \left[ w + \frac{(\overline{\rho'w'})}{\rho} \right] \frac{\partial v}{\partial \zeta} - K_1 uv + K_2 u^2 \\ = -\frac{1}{\rho h_2} \frac{\partial p}{\partial \eta} + \frac{1}{\rho} \frac{\partial}{\partial \zeta} \left[ \mu \frac{\partial v}{\partial \zeta} - \rho(\overline{v'w'}) \right], \end{aligned} \quad (4)$$

$$0 = \frac{\partial p}{\partial \zeta},$$

$$\frac{\partial}{\partial \xi} (\rho h_2 u) + \frac{\partial}{\partial \eta} (\rho h_1 v) + \frac{\partial}{\partial \zeta} \left\{ \rho h_1 h_2 \left[ w + \frac{(\overline{\rho'w'})}{\rho} \right] \right\} = 0, \quad (5)$$

$$\begin{aligned} \frac{u}{h_1} \frac{\partial \bar{H}}{\partial \xi} + \frac{v}{h_2} \frac{\partial \bar{H}}{\partial \eta} + \left[ w + \frac{(\overline{\rho'w'})}{\rho} \right] \frac{\partial \bar{H}}{\partial \zeta} \\ = \frac{1}{\rho} \frac{\partial}{\partial \zeta} \left\{ \mu \left[ \frac{\partial \bar{H}}{\partial \zeta} + \frac{1-\text{Pr}}{\text{Pr}} \frac{\partial}{\partial \zeta} (c_p T) \right] - \rho(\overline{w'\bar{H}'}) \right\}. \end{aligned} \quad (6)$$

Certain terms on the right hand sides of equations (3) and (4), namely

$$\mu \frac{\partial u}{\partial \zeta} - \rho(\overline{u'w'}), \quad \mu \frac{\partial v}{\partial \zeta} - \rho(\overline{v'w'})$$

consist of shear stress terms  $\mu(\partial u/\partial \zeta)$  and  $\mu(\partial v/\partial \zeta)$  together with Reynolds stresses  $-\rho(\overline{u'w'})$  and  $-\rho(\overline{v'w'})$ . We will denote their values by  $\tau_1$  and  $\tau_2$  and their values at the surface of the body by  $\tau_{01}$  and  $\tau_{02}$ .

It will be seen that the first three equations are similar to laminar equations, except that  $w$  is replaced by  $w + (1/\rho)(\overline{\rho'w'})$  and the terms on the right hand side of the equations which in laminar flow would be  $\mu(\partial u/\partial \zeta)$  and  $\mu(\partial v/\partial \zeta)$  are  $\tau_1$  and  $\tau_2$ . The energy equation (6) also resembles the laminar flow energy equation, except that it has an additional term  $-\rho(\overline{w'\bar{H}'})$ .

The values of  $\partial p/\partial \xi$  and  $\partial p/\partial \eta$  are obtained from the flow at the edge of the boundary layer. Denoting the values of flow quantities at the edge by the subscript "e" we have

$$\left. \begin{aligned} \frac{u_e}{h_1} \frac{\partial u_e}{\partial \xi} + \frac{v_e}{h_2} \frac{\partial u_e}{\partial \xi} - K_2 u_e v_e + K_1 v_e^2 &= -\frac{1}{\rho h_1} \frac{\partial p}{\partial \xi}, \\ \frac{u_e}{h_1} \frac{\partial v_e}{\partial \xi} + \frac{v_e}{h_2} \frac{\partial v_e}{\partial \eta} - K_1 u_e v_e + K_2 u_e^2 &= -\frac{1}{\rho h_2} \frac{\partial p}{\partial \eta}, \end{aligned} \right\} \quad (7)$$

since  $p$  is unchanged in travelling through the boundary layer along a normal to the surface.

In deriving momentum-integral equations in laminar flow it is usual to eliminate  $w$ , and in addition no direct use is made of the energy equation.

Here we eliminate  $w + (\overline{\rho'w'})/\rho$  and the momentum-integral equations will be the same as those in laminar flow. These equations are derived in Ref.3 and so we shall only give the results here. For reasons given in Ref.3 it is usual to use "streamline co-ordinates" which have the property that the curves  $\eta = \text{constant}$  are the projections on to the surface of the streamlines of the external flow. In these co-ordinates  $v_e = 0$  by definition.

We write

$$\left. \begin{aligned} \delta_1 &= \int_0^\delta \left(1 - \frac{\rho u}{\rho_e u_e}\right) dz, & \delta_2 &= - \int_0^\delta \frac{\rho v}{\rho_e u_e} dz, \\ \theta_{11} &= \int_0^\delta \left(1 - \frac{u}{u_e}\right) \frac{\rho u}{\rho_e u_e} dz, & \theta_{12} &= \int_0^\delta \left(1 - \frac{u}{u_e}\right) \frac{\rho v}{\rho_e u_e} dz, \\ \theta_{21} &= - \int_0^\delta \frac{\rho uv}{\rho_e u_e^2} dz, & \theta_{22} &= - \int_0^\delta \frac{\rho v^2}{\rho_e u_e^2} dz. \end{aligned} \right\} \quad (8)$$

Finally we assume the external flow to be irrotational, so that a velocity potential exists, which we may put equal to  $\xi$ . It can be shown that in this case  $h_1 = 1/u_e$ .

The momentum-integral equations then become



$$\frac{1}{\rho_e} \frac{\partial}{\partial \xi} (\rho_e \theta_{11}) + \frac{1}{h_2 \rho_e u_c} \frac{\partial}{\partial \eta} (\rho_e \theta_{12}) + \frac{1}{u_e} \frac{\partial u_e}{\partial \xi} (2\theta_{11} + \delta_1) - \frac{1}{u_e} K_1 (\theta_{11} - \theta_{22}) = \frac{\tau_{01}}{\rho_e u_e^3}, \quad (9)$$

$$\frac{1}{\rho_e} \frac{\partial}{\partial \xi} (\rho_e \theta_{21}) + \frac{1}{h_2 \rho_e u_c} \frac{\partial}{\partial \eta} (\rho_e \theta_{22}) + \frac{2}{u_e} \frac{\partial u_e}{\partial \xi} \theta_{21} + \frac{1}{h_2 u_c^2} \frac{\partial u_e}{\partial \eta} (\theta_{11} + \theta_{22} + \delta_1) - \frac{2}{u_e} K_1 \theta_{21} = \frac{\tau_{02}}{\rho_e u_e^3}, \quad (10)$$

as shown in Ref. 3.

## 2.2 Three-dimensional effects

An account of the general behaviour of three-dimensional boundary layers (whether laminar or turbulent) is given in Ref. 3, and we shall not repeat this in detail. However we may mention some of the more important points.

As we traverse the boundary layer along a normal to the surface the direction of flow changes; the velocity vector rotates usually, but not always, in one direction as we travel from outside towards the surface. If we take the direction of the external flow as the standard direction, any component of velocity normal to this direction will be called "cross-flow".

A physical explanation for the existence of cross-flows may be given as follows. The streamlines at the edge of the boundary layer are supposed to be curved, so that there must be an inward pressure gradient balancing the centrifugal force. Near to the surface of the body the fluid has been retarded, whilst the pressure gradient is unchanged. Hence the inwards pressure gradient is now too great for the centrifugal force and the fluid is made to move inwards.

This is fairly easy to understand so long as the inwards pressure gradient increases as we travel downstream. When it decreases and changes sign, as it will do if the external streamlines reduce their curvature and bend the other way as at a point of inflexion, the matter is more complicated. The reduction, vanishing, and reversal of the pressure gradient does not cause an immediate reduction, vanishing and reversal of the cross-flow. This takes time. The reversal first occurs downstream of the point of inflexion and then only near to the body, so that there are places where the cross-flow is inwards (referred to the new curvature) at points near to the body, and outwards at points further away. Only after travelling some distance downstream of the point of inflexion will the flow be reversed at all levels of the boundary layer. Fig. 1 shows some calculated cross-flow components for a laminar boundary layer. Similar cross-flows should appear if the boundary layer is turbulent.

In general the cross-flow in a turbulent boundary layer is much less than in one which is laminar. This is to be expected since in equations (1) and (2) the virtual shear stress terms such as

$$\mu \frac{\partial u}{\partial \zeta} - \rho(\overline{u'w'}), \quad \mu \frac{\partial v}{\partial \zeta} - \rho(\overline{v'w'})$$

are much larger, particularly at high Reynolds numbers, than the corresponding shear stress terms  $\mu(\partial u/\partial \zeta)$  and  $\mu(\partial v/\partial \zeta)$  in laminar flow. The effect of this shear stress is to resist the growth of cross-flow. The reduction is well illustrated in Fig. 2 taken from Ref. 13. This shows oil-flow patterns over a wing with 55° sweep. The oil-flow lines lie along the direction of flow close to the surface of the wing. The direction of flow outside the boundary layer may be taken to be almost the same as that of the undisturbed flow. It will be seen that there are wedge-shaped areas where the direction of flow is much "straighter" than over the rest of the wing. These are places where the flow is turbulent and at these places the cross-flow is much less than at places where the flow is laminar. In general one may expect turbulent mixing to attempt to maintain the mainstream velocity in magnitude and direction deeper down into the boundary layer than in laminar flow. The fact that this happens to the magnitude of the velocity vector is well-known from studies in two dimensions. It will also happen to the direction of the vector.

Another major effect of the three-dimensional nature of the flow is more familiar since it occurs in axially symmetric flow. This is the effect of diverging or converging streamlines in the external flow. Converging streamlines cause a thickening of the boundary layer. This is to be expected, since the boundary layer has less room to "spread itself", so to speak, over the surface in the converging flow. The opposite effect takes place when the streamlines diverge.

### 2.3 The axially symmetric analogy<sup>14</sup>

Let us suppose that we are following a definite external streamline  $\eta = \text{constant}$ , along which we have

$$ds = h_1 d\xi = \frac{1}{u_e} d\xi$$

and so along this streamline

$$\frac{\partial}{\partial \xi} = \frac{1}{u_e} \frac{\partial}{\partial s}. \quad (11)$$

In addition we write  $H = \delta_1/\theta_{11}$ ,  $h_2 = r$  and denote partial derivatives with respect to  $s$  by primes.

We now assume that the crosswise component of velocity and its derivatives are small. In this case we find that equations (9) and (10) reduce to

$$\theta'_{11} + \theta_{11} \left\{ (H + 2) \frac{u'_e}{u_e} + \frac{r'}{r} + \frac{\rho'_e}{\rho_e} \right\} = \frac{\tau_{01}}{\rho_e u_e^2}, \quad (12)$$

$$\theta'_{21} + \theta_{21} \left\{ \frac{\rho'_e}{\rho_e} + \frac{2u'_e}{u_e} + \frac{2r'}{r} \right\} + \frac{1}{ru_e} \frac{\partial u_e}{\partial \eta} (\theta_{11} + \delta_1) = \frac{\tau_{02}}{\rho_e u_e^2}. \quad (13)$$

It will be seen that equation (12) is the standard momentum-integral equation for compressible flow over an axisymmetric body, whose cross sections have radius  $r$ . This is what we mean when we speak of the axially symmetric analogy.

Equation (12) is identical to the well-known two-dimensional equation with  $u'_e/u_e$  replaced by

$$\frac{u'_e}{u_e} + \frac{1}{H + 2} \frac{r'}{r}. \quad (14)$$

Now  $r'/r$  (as in axisymmetric flow) is a measure of the amount the streamlines diverge (or converge if  $r'$  is negative). Thus it is seen that converging flow ( $r' < 0$ ) has the same effect on  $\theta_{11}$  as an adverse pressure gradient.

In a calculation it is necessary to determine the value of  $r$ . It can be shown<sup>14,15</sup> that if the equation of the surface in Cartesian co-ordinates is  $z = z(x, y)$  and if  $U$  and  $V$  are velocity components parallel to the axes  $x$  and  $y$ , then  $r$  is given by

$$u_e \frac{\partial}{\partial s} \left( \log \frac{u_e^2 r^2}{g} \right) = 2 \left( \frac{\delta U}{\delta x} + \frac{\delta V}{\delta y} \right), \quad (15)$$

where

$$u_e \frac{\partial}{\partial s} = U \frac{\delta}{\delta x} + V \frac{\delta}{\delta y}, \quad (16)$$

$$\frac{\delta}{\delta x} = \frac{\partial}{\partial x} + z_x \frac{\partial}{\partial z}, \quad \frac{\delta}{\delta y} = \frac{\partial}{\partial y} + z_y \frac{\partial}{\partial z}, \quad g = 1 + z_x^2 + z_y^2.$$

Subscripts attached to  $z$  denote partial derivatives.

In many cases  $z_x$  and  $z_y$  are small, and in this case equations (15) and (16) simplify to

$$\left. \begin{aligned} u_e \frac{\partial}{\partial s} (\log u_e r) &= \frac{\partial U}{\partial x} + \frac{\partial V}{\partial y}, \\ u_e \frac{\partial}{\partial s} &= U \frac{\partial}{\partial x} + V \frac{\partial}{\partial y}. \end{aligned} \right\} \quad (17)$$

Certain conditions are necessary in order that  $v$  may be small. If terms of order  $v^2$  are ignored we find from equations (3) and (7) that in streamline co-ordinates

$$\begin{aligned} \rho \left\{ u \frac{\partial v}{\partial s} + \left[ w + \frac{(\overline{v'w'})}{\rho} \right] \frac{\partial v}{\partial \zeta} - K_1 uv \right\} \\ = K_2 (\rho_e u_e^2 - \rho u^2) + \frac{\partial}{\partial \zeta} \left[ \mu \frac{\partial v}{\partial y} - \rho(\overline{v'w'}) \right]. \end{aligned} \quad (18)$$

Hence if  $v$  and  $(\overline{v'w'})$  and their derivatives are to be small either  $K_2$  or  $\rho_e u_e^2 - \rho u^2$  must be small. The former condition implies that the geodesic curvature of the streamlines must be small, as might be expected. However  $K_2$  need not be small if  $\rho_e u_e^2 - \rho u^2$  is small. According to Vaglio-Laurin<sup>12</sup> this condition will hold at moderate Mach numbers if the wall is highly cooled. Vaglio-Laurin supposes that  $\rho_e u_e^2 = \rho u^2$  and points out that equation (18) will then admit the solution  $v \equiv 0$ ,  $(\overline{v'w'}) \equiv 0$ . He is then able to use the axially symmetric analogy completely and has no cross-flow equation to solve.

### 3 VELOCITY PROFILES AND SKIN FRICTION COMPONENTS

In order to make an attempt to solve the momentum-integral equations (the solution of the full turbulent boundary layer equations cannot be achieved at present, even in two dimensions) it is necessary to make some assumptions about the velocity profiles and the values of  $\tau_{O1}$  and  $\tau_{O2}$ . These must depend on experiments not many of which have been made in genuinely three-dimensional cases. Boundary layer measurement is a tedious and time-consuming affair, and the determination of  $\tau_{O1}$  and  $\tau_{O2}$  in particular, is a matter of considerable difficulty. So far as I am aware no three-dimensional floating element experiments have ever been made. Preston or Stanton tubes may be used, of course, provided they can be properly calibrated, but their directional properties are poor, so that they may only be expected to give the total skin friction. Oil-flow patterns can of course be used to give direction of flow, but no systematic tests of this nature have been made, so far as I am aware.

Some measurements of velocity profiles have been reported but these are not very numerous. The experiments of Gruschwitz<sup>16</sup> were made in a curved

channel with an initial straight portion. Kuethe, McKee and Curry<sup>17</sup> investigated flow over an elliptic wing swept at an angle of 25°. In these experiments the cross-flow was quite large in places. Wallace<sup>18</sup> made measurements on a swept tapered wing, the mean sweep being 30°, whilst Brebner and Wyatt<sup>13</sup> investigated wings swept at angles of 45° and 55°. Johnston's<sup>5,6</sup> experiments were carried out over a flat wall bounding a jet flowing at right angles against a wall. See Fig.3. Blackman and Joubert<sup>19</sup> examined profiles near to the trailing edge of a delta wing at incidence.

It is from this rather small body of experiment that workers have attempted to develop calculation methods.

### 3.1 Velocity profiles

Calculation methods have so far only been applied to the case of small cross-flow and in this case it is to be hoped that streamwise velocity profiles may be similar to those in two dimensions. Experimental evidence confirms this in general. It has therefore been usually assumed that the streamwise component follows a power law of the form

$$\frac{u}{u_e} = \left(\frac{z}{\delta}\right)^{\frac{1}{n}} \quad (19)$$

and  $n = 7$  is commonly used both for subsonic and supersonic flows. Mager<sup>20</sup> found that this form fitted some experiments of Gruschwitz<sup>16</sup> fairly well.

Cooke<sup>21</sup> found that the form

$$\frac{u}{u_e} = \left(\frac{z}{\delta}\right)^{\frac{1}{2}(H-1)} \quad (20)$$

fitted some experiments of Wallace<sup>18</sup> quite well except near to the wall. Becker<sup>22</sup> also used this form.

Zaat<sup>23</sup> suggested for compressible flow

$$\left. \begin{aligned} \frac{u}{u_e} &= \left\{ 1 + k \left( 1 - \frac{z}{\delta} \right) \right\} \left( \frac{z}{\delta} \right)^k, \\ \frac{v}{u_e} &= \left( a + b \frac{z}{\delta} \right) \left( 1 - \frac{z}{\delta} \right)^2 \frac{u}{u_e}, \end{aligned} \right\} \quad (21)$$

where

$$a = \tan \alpha = \frac{\tau_{02}}{\tau_{01}}.$$

He quoted Wallace's<sup>18</sup> experiments to justify the form for  $v/u_e$ .

The form, based on experiments by Gruschwitz<sup>16</sup> on ducts and Wallace<sup>18</sup> on wings,

$$\frac{v}{u_e} = \left(1 - \frac{\zeta}{\delta}\right)^2 \frac{u}{u_e} a, \quad (22)$$

with  $a = \tan \alpha$ , was used by Mager<sup>20</sup>, Braun<sup>24</sup> and Cooke<sup>21</sup>, whilst Becker<sup>22</sup> suggested that

$$\frac{v}{u_e} = \left\{1 - \left(\frac{u}{u_e}\right)^2\right\} \frac{u}{u_e} a \quad (23)$$

fitted Gruschwitz's experiments very well if

$$a = \frac{4}{3} \tan \alpha = \frac{4}{3} \frac{\tau_{02}}{\tau_{01}}. \quad (24)$$

Equation (22) also fits the experiments of Kuethe et al.<sup>17</sup> quite well, but (19) fits poorly with  $n = 7$ .

Johnston<sup>5,6</sup> made a close study of the velocity profiles of references 16 and 17 and as a result of this and of a long series of experiments of his own he suggested a form for the cross-flow as shown in Fig. 4. It will be seen that  $v/u_e$  is expressed as a function of  $u/u_e$ , so that  $v = 0$  when  $u/u_e = 0$  and also when  $u/u_e = 1$ . Fig. 5, reproduced from Ref. 5, shows how Johnston's model fits the data of Kuethe et al. This form of plot does not show very clearly the way the cross-flow varies across the boundary layer. We have therefore in Fig. 6 plotted  $v/u_e$  as a function of  $\zeta/\delta$  for Johnston's fit of his model to one of the profiles of Gruschwitz<sup>16</sup> (station 10 along line 3), taking for the streamwise component the value

$$\frac{u}{u_e} = \left(\frac{\zeta}{\delta}\right)^{\frac{1}{7}},$$

which fits the observations quite well. This particular profile was chosen because in most of the others the peak is too near to the  $v/u_e$  axis to be conveniently drawn. Profiles such as that in Fig. 6 illustrate the difference

between laminar and turbulent boundary layers in this respect. The peak is very much nearer to the wall in the turbulent than in the laminar case. Fig. 7 is an attempt to give a full three-dimensional picture of the same profile. Unfortunately Johnston's model differs from others mostly in the region close to the wall where measurements are the most difficult to make and suffer from the most inaccuracy.

Johnston's form for the velocity profile  $v$  may be written

$$\frac{v}{u_e} = \frac{eu}{u_e} \quad (25)$$

near to the wall, and

$$\frac{v}{u_e} = A \left( 1 - \frac{u}{u_e} \right) \quad (26)$$

further away from the wall. The change from one to the other takes place where the two lines in the  $u, v$  plane (Fig. 4) intersect. Johnston suggests that for external streamlines which are initially straight and then become circular  $A$  is given by

$$A = 2\beta, \quad (27)$$

where  $\beta$  is the angle through which the streamlines have turned. He found, however, that except perhaps for flow in ducts, one cannot rely on the factor 2 in equation (27). Indeed a factor 1 gave closer agreement in one case and this was the number he used in a calculation. The quantity  $e$  is equal to  $\tan \alpha$  as already defined ( $\alpha$  is the angle between streamlines and limiting streamlines) and is an unknown to be determined in the course of a calculation.

Finally, Coles<sup>3</sup> suggested that the velocity vector  $\underline{q}$  should be given by

$$\underline{q} = \underline{q}_f + \underline{q}_w,$$

where

$$\underline{q}_f = \underline{q}_\tau f\left(\frac{\zeta q_\tau}{v}\right), \quad \underline{q}_w = \frac{\Pi q_\tau}{\kappa} w\left(\frac{\zeta}{\delta}\right).$$

In these equations  $q_\tau$  is the magnitude of a friction velocity vector  $\underline{q}_\tau$  which is taken parallel to the surface shear stress vector  $\underline{\tau}$ . The

functions  $f$  and  $w$  are the well-known "law of the wall" and "law of the wake" functions, that is

$$f\left(\frac{\zeta q_{\tau}}{\nu}\right) = \frac{1}{k} \ln\left(\frac{\zeta q_{\tau}}{\nu}\right) + c, \quad (28)$$

and  $w$  is a function tabulated by Coles. According to Coles  $\underline{q}_{\tau}$  is to be a vector constant in magnitude and direction at any given station. Thus  $\underline{q}_{\tau}$  and  $\underline{q}_w$  are both vectors constant in direction but varying in magnitude for varying  $\zeta$  according to the variations of the functions  $f$  and  $w$ .  $\underline{q}$  itself varies both in magnitude and direction. Coles finds in an example that the direction of  $\underline{q}_w$  is nearly the same as the direction of the external pressure gradient at the point concerned, and makes the tentative suggestion that this should hold universally.

Blackman and Joubert<sup>19</sup> attempted to test the theory in an experiment. They divided the vector  $\underline{q}_w$  into components  $w_h$  in the  $\underline{q}_{\tau}$  direction and  $w_j$  perpendicular to this.  $w_h$  and  $w_j$ , suitably normalised, should both have the shape of the law of the wake function  $w(\zeta/\delta)$  if the hypothesis of Coles is correct. The results are shown in Fig. 8. Blackman and Joubert claim that the fit is good, since  $w_j$  has a fairly good fit. They rightly say that  $w_h$  is subject to much more uncertainty than  $w_j$ ; indeed the lack of experimental precision obtainable by present methods makes scatter inevitable in this component. There was, however, very little cross-flow in the experiments ( $\alpha < 5^\circ$ ) and it was not possible to determine the direction of the pressure gradient, which was in any case small.

The question of the fit of experiments to the models of Coles<sup>4</sup> and Johnston<sup>5</sup> is in a state of some confusion. Coles found that his model fitted the measurements of Kuethe et al<sup>17</sup> very well, and Johnston has used Fig. 5 to show how his model also fits the same observations. On the other hand Johnston found that his own observations could not be made to fit Coles's model. Johnston was able to fit his model fairly well to the experiments of Gruschwitz<sup>16</sup>; Coles felt that the experiments concerned were probably subject to errors near to the wall. In the discussion following Ref. 6 Coles reported on his attempts to fit Johnston's measurements to Coles's model. He found that  $\underline{q}_{\tau}$  could be made to fit well, and that the direction of  $\underline{q}_w$  was close to the direction of the pressure gradient, but that the fit to his form for  $w(\zeta/\delta)$  was not good. Finally we may note that the profiles of Blackman and Joubert<sup>19</sup> helped to confirm Coles's model but could not be made to fit that of Johnston.

Much less is known about three-dimensional compressible boundary layer profiles than incompressible ones. One may hope that two-dimensional flows will again give us a guide. In this connection one may expect that the transformation



$$z = \int_0^{\zeta} (\rho/\rho_m) d\zeta, \quad \Delta = \int_0^{\delta} (\rho/\rho_m) d\zeta,$$

where  $\rho_m$  is evaluated at the temperature  $T_m$  of equation (31) below, will reduce streamwise compressible profiles to incompressible ones. Spence<sup>25</sup> found this transformation to be most successful in the two-dimensional case. More speculative would be to assume that the transformation would also hold for the cross-flow. If it did one would be able to formulate a compressibility correlation similar to that for laminar flow.

### 3.2 Wall friction values

For the streamwise skin friction in incompressible flow Becker<sup>22</sup> used the Ludwig-Tillman formula<sup>26</sup>.

$$\frac{\tau_{01}}{\rho_e u_e^2} = 0.123 \times 10^{-0.678} \left( \frac{u_e \theta_{11}}{\nu} \right)^{-0.268}. \quad (29)$$

Cooke<sup>30</sup>, following Spence<sup>27</sup> used the relation

$$\frac{\tau_{01}}{\rho_e u_e^2} = 0.0088 \frac{\rho_m}{\rho_e} \left( \frac{\rho_e u_e \theta_{11}}{\mu_m} \right)^{-\frac{1}{5}}, \quad (30)$$

where quantities with suffix m are evaluated at a temperature  $T_m$  determined from the relation

$$T_m = \frac{1}{2}(T_e + T_r) + 0.22(T_r - T_e), \quad (31)$$

where  $T_r$  is the recovery temperature given by

$$T_r = T_e \left\{ 1 + \frac{1}{2} \bar{r} (\gamma - 1) M_e^2 \right\}. \quad (32)$$

$\bar{r}$  is the "recovery factor" and is usually taken as 0.89, whilst  $M_e$  is the Mach number at the edge of the boundary layer. The assumption

$$\mu \propto T^\omega$$

was also made, with  $\omega = 8/9$ .

Braun<sup>24</sup> used the relation

$$\frac{\tau_{01}}{\rho_e u_e^2} = K \left( \frac{\mu_m}{\mu_e} \right)^{\frac{1}{4}} \left( \frac{T_e}{T_m} \right)^{\frac{3}{4}} \left( \frac{v_e}{u_e \delta} \right)^{\frac{1}{4}}, \quad (33)$$

with  $T_m$  given by equation (31). The viscosity temperature relation used was

$$\frac{\mu}{\mu_e} = C \frac{T}{T_e}. \quad (34)$$

$K$  is 0.0225 for a flat plate. Braun, who was dealing with a slightly yawed cone, did not take  $K = 0.0225$  but he multiplied this value by  $2/\sqrt{3}$ , saying that this is usually done for an unyawed cone.

All these forms are taken from two-dimensional methods. The only evidence for this comes from axisymmetric bodies, for which it seems to be true that the same flow mechanism holds locally as in two-dimensional bodies.

Vaglio-Laurin<sup>12</sup>, in a problem with zero cross-flow, after using a transformation which reduce his compressible problem to an incompressible axially symmetric one with zero pressure gradient, uses equation (28) which, on integration of the equation for  $\theta_{11}$  in equation (8) gives  $\tau_{01}$  in terms of  $\theta_{11}$ .

The skin friction component  $\tau_{02}$  in all the methods is taken to be equal to  $\tau_{01} \tan \alpha$ , where  $\alpha$  is to be determined in the course of the solution. All workers except Becker take

$$\tan \alpha = \lim_{z \rightarrow 0} \frac{v}{u}. \quad (35)$$

Becker<sup>22</sup> inserts a factor  $\frac{3}{4}$  on the right of equation (35). There is no special reason why equation (35) should hold exactly, since the forms for  $u$  and  $v$  used by all workers do not apply near to the wall.

#### 4. GENERAL METHODS

Only two general methods of solution seem to have been suggested, both of which assume small cross-flow and both of which solve the streamwise equations by taking over two-dimensional methods. Braun<sup>24</sup>, who found a solution

for a cone at small angles of yaw, also implicitly assumed small cross-flow and used two-dimensional properties for the streamwise flow. Vaglio-Laurin<sup>12</sup> of course took the cross-flow equal to zero and then also used two-dimensional methods for the streamwise flow.

#### 4.1 Cooke's method<sup>21</sup>

In this method the solution of the streamwise equation follows closely the method of Spence<sup>27</sup> in two dimensions. This method uses the momentum equation (12) and in incompressible flow the streamwise shear stress is given by

$$\frac{\tau_{01}}{\rho u_e^2} = 0.0088 \left( \frac{u_e \theta_{11}}{\nu} \right)^{-1/5}. \quad (36)$$

This equation is due to Young<sup>28</sup>.

Writing

$$\Theta = \theta_{11} \left( \frac{u_e \theta_{11}}{\nu} \right)^{1/5}$$

and assuming that in the determination of  $\theta_{11}$  it is sufficiently accurate to write  $H = 1.5$ , we find that equation (12) becomes in the incompressible case

$$\frac{\partial}{\partial s} \left\{ \Theta u_e^4 r^{1.2} \right\} = 0.0106 u_e^4 r^{1.2}, \quad (37)$$

where  $r$  is found from equation (17).

For the cross-flow the form (22) is assumed, with  $a = \tan \alpha \approx \alpha$ , and  $H$  is again assumed to be constantly equal to 1.5. Writing

$$\varepsilon = \alpha r u_e^{-3/2}.$$

Cooke finds

$$\frac{d\varepsilon}{ds} + \frac{0.0166}{\Theta} \varepsilon = \frac{2.187}{u_e^{2.5}} \frac{\partial u_e}{\partial \eta}.$$

This method was applied to a  $55^\circ$  swept wing tested by Brebner and Wyatt<sup>13</sup>, and included the determination of  $H$  by Spence's method<sup>29</sup>, and so  $\theta_{11}$ ,  $\delta_1$  and  $\beta$  could all be calculated. Some results are shown in Figs.9 and 10.

The method can readily be extended to compressible flow using a transformation for the streamwise flow due to Spence<sup>27</sup>. For the flow over infinite yawed wings the equations for  $\theta_{11}$  in the case of zero heat transfer and also of constant wall temperature are given in Ref. 30.

Cooke<sup>31</sup> has also applied this method to the flow over a delta wing of 13% thickness-chord ratio at zero lift at a Mach number of 2. This wing has been tested in the R.A.E. 8 foot tunnel and it was found that the pressure measurements agreed quite well with calculations by slender thin wing theory. However the separate velocity components were not measured and so the calculated values of these components were used in the boundary layer calculations. The streamlines could then be found and are drawn in Fig. 11. Turbulent streamwise calculations using equation (12) and Spence's transformation<sup>27</sup> were then made. These calculations could be simplified because it was found that the term  $(H + 2) (u'_e/u_e) + \rho'/\rho$  could be ignored compared with the other terms in the coefficient of  $\theta_{11}$ . The result is shown in Fig. 12. There is considerable convergence of the external streamlines near to the centre line and this causes a thickening of the boundary layer in this region. Everywhere else it was found that the value of  $\theta_{11}$  was much the same as it would have been if the flow had been over a flat plate of the same planform. It was found also that the additional pressure drag due to the displacement thickness was less than 1% of the total skin friction drag plus wave drag and it could therefore be ignored.

#### 4.2 Becker's method<sup>22</sup>

Becker assumes the equations (20) and (23) for the velocity components. For the streamwise shear stress he assumes the well-known Ludwig and Tillman relation<sup>26</sup>

$$\frac{\tau_{01}}{\rho u_e^2} = 0.123 \times 10^{-0.678H} \left( \frac{u_e \theta_{11}}{\nu} \right)^{-0.268},$$

and suggests that a close approximation to this is

$$\frac{\tau_{01}}{\rho u_e^2} = 0.0125 \left( \frac{u_e \theta_{11}}{\nu} \right)^{-1/4}. \quad (38)$$

He deals only with incompressible flow.

Unfortunately Becker assumes a rather special external flow corresponding to a special value of  $r$  in equation (12) namely  $r = 1/u_e$ . This assumption is equivalent to assuming that  $\partial w_e / \partial \zeta = 0$ , which implies that the external flow is two-dimensional, as may be seen by consideration of the equation of continuity for the external flow. The assumption is easily avoided and Becker's streamwise equation may then be written

$$\theta'_{11} + \theta_{11} \left\{ (H+2) \frac{u'_e}{u_e} + \frac{r'}{r} \right\} = 0.123 \times 10^{-0.678H} \left( \frac{u_e \theta_{11}}{\nu} \right)^{-0.268}. \quad (39)$$

The cross-flow equation (13) becomes according to Becker

$$\theta'_{21} + \theta_{21} \left\{ Y_3(H) \frac{\tau_{01}}{\theta_{11} \rho u_e^2} + \frac{2u'_e}{u_e} + \frac{2r'}{r} \right\} = -\frac{1}{ru_e} \frac{\partial u_e}{\partial \eta} (1+H) \theta_{11}, \quad (40)$$

where

$$Y_3(H) = \frac{3}{4} \frac{2H-1}{H+1},$$

though Becker's equation has the term  $2r'/r + 2u'_e/u_e$  missing because of his special value of  $r$ .

In order to solve these equations one may assume a constant value of  $H$  as we did previously. Becker suggests  $H = 1.29$  in one example. This makes  $Y_3(H) = 0.52$ . As an alternative Becker finds  $H$  by an equation which is independent of  $r$ . He writes

$$\bar{\omega} = 1 - \left[ \frac{H-1}{H(H+1)} \right]^{H-1}$$

and uses the equation

$$\theta_{11} \left( u_e \bar{\omega}^2 \right)^1 + A u_e \bar{\omega}^2 = B u_e^2 \quad (41)$$

due to Kehl<sup>32</sup>, where

$$A = 0.00894,$$

$$B = \frac{0.0164}{\log(u_e \theta_{11} / \nu)} - \frac{0.85}{u_e \theta_{11} / \nu - 300}$$

Equations (39), (40) and (41) are then three equations for the three unknowns  $\delta$ ,  $H$  and  $\alpha$ , since

$$\theta_{11} = \frac{H-1}{H(H+1)} \delta, \quad \theta_{21} = -\frac{H-1}{H(2H-1)} \alpha \delta. \quad (42)$$

Becker does two examples, the first of which is the case where the streamlines are circles of radius  $R$ , and  $u_e = f(R)$ , so that  $u_e$  is constant along streamlines; he also supposes the boundary layer is "very thick", so that the term  $\tau_{01}$  may be ignored in equation (40). This equation then reduces to

$$\theta'_{21} = \frac{\theta_{11}}{R} (1+H),$$

remembering that Becker writes  $r = 1/u_e$ . If  $H$  and  $\theta_{11}$  are constant, and  $H$  is equal to 1.29 this by equations (42) reduces to

$$\alpha = 1.58\beta,$$

where  $\beta$  is the amount the external streamlines have turned from the start.

For his second example Becker considers the decay of a cross-flow which had developed earlier, specified by  $\theta_{21} = (\theta_{21})_0$ , and is now subject to uniform external flow with straight streamlines. In this case equation (40) becomes

$$\theta'_{21} + \frac{0.0065}{\theta_{11} (\text{Re}_{\theta_{11}})^{1/4}} \theta_{21} = 0,$$

where

$$\text{Re}_{\theta_{11}} = \frac{u_e \theta_{11}}{\nu},$$

and once more  $H = 1.29$ .

This gives, using (38),

$$\theta_{21} = (\theta_{21})_0 e^{-s/\ell},$$

where

$$\ell = 154 \theta_{11} \left( \text{Re} \theta_{11} \right)^{1/4}.$$

#### 4.3 Johnston's solution along a line of symmetry<sup>5,33</sup>

When applying the axially symmetric analogy we assumed that  $\theta_{12}$ ,  $\theta_{22}$  and their derivatives in equation (9) could be ignored. Johnston, though he ignores  $\theta_{22}$  (it is in fact zero along a line of symmetry), does not ignore  $\partial\theta_{12}/h_2\partial\eta$ .

If we assume constant density and write

$$h_2 = r, \quad \delta_1 = H \theta_{11}$$

we find that equation (9) takes the form

$$\theta'_{11} + \frac{1}{r} \frac{\partial \theta_{12}}{\partial \eta} + \theta_{11} \left\{ (H+2) \frac{u'_e}{u} + \frac{r'}{r} \right\} = \frac{\tau_{01}}{\rho_e u_e^2}, \quad (43)$$

which we may compare with equation (12). Johnston points out that the term  $r'\theta_{11}/r$  represents the effect of converging or diverging streamlines (as we have already explained in Section 2.3) and that the term  $\partial\theta_{12}/r\partial\eta$  represents the effect of boundary layer "skewing". That this term need not be small was shown by Moore and Richardson<sup>34</sup>. In one experiment, for instance, they found the values

$$\frac{1}{r} \frac{\partial \theta_{12}}{\partial \eta} = 0.007, \quad \theta_{11} (H+2) \frac{u'_e}{u} = -0.008, \quad \frac{\tau_{01}}{\rho_e u_e^2} = 0.0017,$$

so that in this case the contribution of  $\partial\theta_{12}/r\partial\eta$  certainly could not be ignored.

Using his model {equations (25) and (26)} for the velocity profiles Johnston shows that for large Reynolds numbers ( $Re_{\theta_{11}} > 10^4$ )

$$\theta_{12} = A (\theta_{11} - \delta_1).$$

Hence we have along a line of symmetry

$$\frac{1}{r} \frac{\partial \theta_{12}}{\partial \eta} = \frac{1}{r} \frac{\partial A}{\partial \eta} (\theta_{11} - \delta_1). \quad (44)$$

Now, as discussed in section 3.1 Johnston assumes that  $A = \beta$ , where  $\beta$  is the angle the streamlines have turned from their initial straight path, and since the curvature  $K_1$  of the lines  $\xi = \text{constant}$  is

$$\frac{1}{r} \frac{\partial \beta}{\partial \eta}$$

we have by equation (2)

$$K_1 = -\frac{r'}{r} = \frac{1}{r} \frac{\partial \beta}{\partial \eta} = \frac{1}{r} \frac{\partial A}{\partial \eta}. \quad (45)$$

Finally Johnston assumes that  $r = 1/u_e$ , the same assumption that was used by Becker<sup>22</sup>, which is tantamount to assuming that the external flow is two-dimensional and is probably justified for the experiment of Fig. 3.

Hence we have from equations (43), (44) and (45)

$$\theta'_{11} = -2\theta_{11} \frac{u'_e}{u_e} + \frac{\tau_{01}}{\rho_e u_e^2} \quad (46)$$

along a line of symmetry.

This equation is integrated by using the Ludwig and Tillman<sup>26</sup> formula for  $\tau_{01}$  combined with the von Doenhoff and Tetervin<sup>35</sup> formula for  $H$ . Alternatively a method due to Rotta<sup>36</sup> is followed.

Either of the methods gives results agreeing well with experiment in the special case considered.



#### 4.4 Braun's solution for the slightly yawed cone<sup>24</sup>

Braun solves the problem of a cone of semi-angle  $\Theta$  yawed at a small angle  $\gamma$  in a supersonic stream. He uses a streamline co-ordinate system and uses the velocity profiles (19) and (22) and wall shear stress values given by equations (33), (31) and (32) for  $\tau_{01}$  and (35) for  $\tau_{02}$ . For the external flow he uses Kopal's tables<sup>37</sup>. Writing  $\lambda = \gamma/\sin \Theta$  for the yaw parameter he expands  $\tan \alpha$  and  $\delta$  in the form

$$\tan \alpha = \alpha_1 \lambda + \alpha_2 \lambda^2 + \dots,$$

$$\delta = \delta_0 + \delta_1 \lambda + \dots .$$

He is then able to find  $\alpha_1$ ,  $\delta_0$  and  $\delta_1$  in closed form. Perhaps the most interesting results are the deflection of the limiting streamlines, that is, the value of  $\alpha$  to the first order in  $\lambda$ . Fig. 13 is taken from Braun's paper. In this figure  $\psi$  is the azimuth angle round the cone measured from the generator with the greatest inclination to the flow at infinity. It will be seen that  $\alpha$  is increased by heating, but raising the Mach number reduces it. The deflection angle is much smaller than in the laminar adiabatic case and it decreases with Mach number in contrast to the laminar case, where it increases with Mach number for values of Mach number greater than about 2.

#### 5 TRANSITION

We shall only make a few isolated remarks in this section, some of which are speculative and not completely justified either experimentally or theoretically.

So far no calculations appear to have been made in cases when the flow is partly laminar and partly turbulent. First of all the determination of the transition "front" itself is a difficult matter into which we shall not enter, beyond remarking that two kinds of instability seem to be involved, namely two-dimensional instability (Tollmien-Schlichting) and sweep instability. It was suggested by Eichelbrenner and Michel<sup>38</sup> that both of these types exist on a surface; in certain regions one is more important than the other and in other regions their roles are reversed. Thus, for a slender wing with leading edge separation and reattachment, transition fronts as shown in Fig. 14 may be possible<sup>39</sup>, where CDE is a front due to two-dimensional instability and ABC and EFG are fronts due to sweep instability. Fronts of this type have been observed. A third type of instability, that described by Görtler<sup>40</sup> as occurring in flow over concave surfaces, may also have its effect in places.

Another interesting fact has been pointed out by Gregory<sup>41</sup>. It is that when transition occurs at an isolated point (say near to the leading edge of a swept wing) the usual wedge of turbulence appears, spreading out at the usual angle, but the wedge is curved, its edges being the envelopes of lines making angles  $\pm 10.6^\circ$  with the external streamlines starting from the point concerned. Fig. 15, taken from Ref. 42, shows calculated wedges of turbulence starting from points at different distances from the leading edge. It will be seen that the nearer the disturbance is to the attachment line the greater the area covered by the turbulence wedge. In particular, if  $x/c$  is equal to 0.01 the whole wing outboard of the point of disturbance is "contaminated". Fig. 16 is taken from photographs by Gregory<sup>42</sup>, and illustrates this phenomenon very well.

When turbulent calculations are to be made they must start with some known initial conditions. In two dimensions it is usual to assume that the

momentum thickness is unchanged at transition; this means that skin friction and displacement thickness are usually discontinuous. (Actually transition does not take place suddenly but is spread over a region which is fairly short, so that skin friction and displacement thickness vary rapidly but are not quite discontinuous.) The assumption is that there is no rapid change in the momentum thickness. An argument in favour of this might run as follows. A discontinuity in momentum thickness implies a sudden change in momentum and this means that there must be not merely a discontinuity in skin friction but also an infinite force at the point of transition. There is some experimental evidence for this assumption, as may be seen from Fig.17 which shows displacement thickness and momentum thickness as drawn by Rotta<sup>43</sup> from experiments by Schubauer and Klebanoff<sup>44</sup>.

In three-dimensional flow the problem is more difficult. An obvious first suggestion is to make  $\theta_{11}$  continuous. This is not sufficient and a second condition is required. One that has been suggested is to make  $\alpha$  continuous, that is, the direction of the limiting streamlines is to be unchanged. Apart from the fact that this direction is connected with skin friction which we expect to be discontinuous, the assumption of an unchanged direction is contrary to the evidence of Fig. 2, a careful examination of which seems to show a discontinuity in direction of the oil-flow lines at the edges of the wedges of turbulence. A discussion which is not, and cannot be, wholly satisfactory, is given in Appendix 1. It would appear from this that the result depends on the angle  $\alpha'$  which the normal to the transition front makes with the local external direction of flow. The result is that

$$\theta_{11} \cos \alpha' - \theta_{12} \sin \alpha' \quad \text{and} \quad \theta_{22} \sin \alpha' - \theta_{21} \cos \alpha'$$

are continuous at transition. If the cross-flow is small,  $\theta_{12}$  is small compared with  $\theta_{11}$  and  $\theta_{22}$  is small compared with  $\theta_{21}$ . In this case the conditions reduce to a simpler form, namely that  $\theta_{11}$  and  $\theta_{21}$  are continuous at transition, independently of the direction of the transition front. This was pointed out to me by Professor A.D. Young.

## 6 CONCLUDING REMARKS

Although little work on turbulent boundary layers has been done the outlook for calculation methods is not quite so dismal as at first appears. Velocity profiles seem to be of a more "universal" shape than in laminar flow, and momentum-integral equations seem to be adequate in favourable or slightly unfavourable pressure gradients. Energy-integral equations could also be further exploited in this connection.

Even in the laminar case it has been found that streamwise velocity profiles are very like two-dimensional ones and, since turbulent mixing is a three-dimensional phenomenon, it may well be expected that this similarity will be borne out more faithfully in the turbulent case. The great difference is that one can never resort to an exact solution to test any method, and experiment is the only possibility. In any case methods are largely empirical. This inevitably means that calculations with turbulent boundary layers will be inaccurate, and indeed in two dimensions an accuracy of from 5 to 10 per cent is all that is usually expected. Within that range the position is not too hopeless and one may well anticipate improvements in the future if only more systematic and careful experiments can be made.

We have made no attempt here to discuss the structure of a three-dimensional turbulent boundary layer. This has an extensive literature in two-dimensions but practically none in three dimensions. In addition, so

far as I am aware, no work has been done in the unsteady case or in connection with separation. The problem of determining separation is difficult enough and doubtful enough even in laminar flow. However separation seems to take place fairly abruptly in the sense that the bending of the streamlines increases considerably just before separation and methods of solution break down when this happens. One may therefore hope that a place where a method breaks down is fairly near to the place of separation. Further than that one cannot go at present.

---

LIST OF SYMBOLS

A	factor in velocity profile (26)
A, B,	factors in equation (41)
a	factor in velocity profiles (21), (22) and (23)
b	factor in velocity profile (21)
C	constant in viscosity temperature relation (34)
c	chord measured normal to leading edge
$c_p$	specific heat at constant pressure
e	factor in velocity profile (25)
$f\left(\frac{\zeta q_\tau}{\nu}\right)$	law of the wall function, eq. (28)
H	form factor
$\bar{H}$	total enthalpy
$h_1, h_2$	coefficients in line element (1)
$K_1, K_2$	geodesic curvatures of curves $\xi = \text{const}$ , $\eta = \text{const}$ . Eq. (2)
K	constant in skin friction formula (33)
M	Mach number
n	power in eq. (19)
p	pressure
Pr	Prandtl number
q	velocity
$q_\tau$	friction velocity
R	radius
$Re_{\theta_{11}}$	Reynolds number based on $\theta_{11}$

LIST OF SYMBOLS (Cont'd)

$\bar{r}$	recovery factor in eq. (32)
$r$	$h_2$
$s$	length measured along a streamline
$T$	temperature
$\bar{T}$	external temperature over unyawed cone. Fig. 13.
$u, v, w$	velocity components
$U_0$	reference velocity
$w_h, w_j$	wake velocity components in direction of limiting streamlines and normal to them
$w(\zeta/\delta)$	law of the wake component
$x, y, z$	Cartesian co-ordinates
$\alpha$	defined by $\tan \alpha = \tau_{02}/\tau_{01}$
$\alpha'$	angle between the normal to the transition front and the local direction of the external flow
$\beta$	angle of turn of external streamlines
$\gamma$	angle of yaw of cone in Braun's work
$\delta$	boundary layer thickness
$\Delta$	transformed boundary layer thickness
$\delta_1, \delta_2$	displacement thickness "components"
$\epsilon$	$\text{aru}_e^{-3/2}$
$\theta_{11}, \theta_{12}, \theta_{21}, \theta_{22}$	momentum thickness "components"
$\Theta$	Fig. 12 and section 4.4. Semi-vertical angle of cone
$\Theta$	Section 4.1. $\theta_{11}(u_e \theta_{11}/\nu)^{1/5}$
$\mu$	coefficient of viscosity
$\nu$	kinematic viscosity
$\xi, \eta, \zeta$	curvilinear co-ordinates, $\xi$ along streamlines, $\zeta$ normal to surface, $\eta$ normal to $\xi$ and $\zeta$
$\rho$	density
$\tau_1, \tau_2$	shear stress components
$\tau_{01}, \tau_{02}$	wall shear stress components
$\psi$	azimuth angle of cone

LIST OF SYMBOLS (Cont'd)

$\omega$  power of T in viscosity-temperature relation

$$\bar{\omega} = 1 - \left[ \frac{H-1}{H(H+1)} \right]^{H-1}$$

Subscript e denotes values at the edge of the boundary layer

" m denotes values at a temperature  $T_m$  given by equation (31)

" r denotes recovery values

---

LIST OF REFERENCES

<u>No.</u>	<u>Author(s)</u>	<u>Title, etc.</u>
1	Sears, W. R.	Boundary layers in three-dimensional flow. Applied Mechanics Reviews, Vol.7, p.281, 1954.
2	Moore, F. K.	Three-dimensional boundary layer theory. Chapter in Advances in Applied Mechanics, Vol. 4. Edited by H.L.Dryden and Th. von Karman, Academic Press, 1956.
3	Cooke, J. C., Hall, M. G.	Boundary layers in three-dimensions. Chap. in Progress in Aeronautical Sciences, Vol. 2. Pergamon Press, 1962.
4	Coles, D.	The law of the wake in the turbulent boundary layer. J. Fluid. Mech., Vol.1, p.191,1956.
5	Johnston, J. P.	The three-dimensional turbulent boundary layer. M.I.T. Gas Turbine Laboratory Report No. 39. 1957.
6	Johnston, J. P.	On the three-dimensional turbulent boundary layer generated by secondary flow. J. of Basic Engineering, Series D, Trans. ASME, Vol. 82, p.233, 1960.
7	Rott, N., Crabtree, L.F.	Simplified laminar boundary-layer calculations for bodies of revolution and for yawed wings. J. Aeron. Sci., Vol. 19, p.553, 1952.
8	Ashkenas, H., Riddell, F. R.	Investigation of the turbulent boundary layer on a yawed flat plate. NACA, TN No. 3383, 1955.
9	Turcotte, D. L.	On incompressible turbulent boundary layer theory applied to infinite yawed bodies. Cornell University Graduate School of Aeronautical Engineering, 1955.
10	Maskell, E. C.	Flow separation in three dimensions. ARC 18,063, 1955.

LIST OF REFERENCES (Cont'd)

- | <u>No.</u> | <u>Author(s)</u>                              | <u>Title, etc.</u>                                                                                                                                                                                      |
|------------|-----------------------------------------------|---------------------------------------------------------------------------------------------------------------------------------------------------------------------------------------------------------|
| 11         | Cooke, J. C.,<br>Brebner, G. G.               | The nature of separation and its prevention by geometric design in a wholly subsonic flow. Chapter in "Boundary Layer and Flow Control". Vol. 1. Edited by G.V. Lachmann, Pergamon Press, London, 1961. |
| 12         | Vaglio-Laurin, R.                             | Turbulent heat transfer in blunt-nosed bodies in two-dimensional and general three-dimensional hypersonic flow. WADC TN 58-301, 1958.                                                                   |
| 13         | Brebner, G. G.,<br>Wyatt, L. A.               | Boundary layer measurements at low speed on two wings of 45° and 55° sweep. ARC C.P. 554. August, 1960.                                                                                                 |
| 14         | Cooke, J. C.                                  | An axially symmetric analogue for general three-dimensional boundary layers. ARC R. and M. No. 3200. June, 1959.                                                                                        |
| 15         | Zaat, J. A.                                   | A simplified method for the calculation of three-dimensional laminar boundary layers. NLL Report F184, 1956.                                                                                            |
| 16         | Gruschwitz, E.                                | Turbulente Reibungsschichten mit Sekundärströmung. Ing. -Arch. Bd. 6, p.355, 1935.                                                                                                                      |
| 17         | Kuethé, A.M.,<br>McKee, P.B.,<br>Curry, W. H. | Measurements in the boundary layer of a yawed wing. NACA TN 1946, 1949.                                                                                                                                 |
| 18         | Wallace, R. E.                                | The experimental investigation of a swept-wing research model boundary layer. Municipal University of Wichita Aerodynamics Report No. 092, 1953.                                                        |
| 19         | Blackman, D. R.,<br>Joubert, P.N.             | The three-dimensional turbulent boundary layer. J. Roy. Aeron. Soc., Vol. 64, p.692, 1960.                                                                                                              |
| 20         | Mager, A.                                     | Generalization of boundary-layer momentum-integral equations to three-dimensional flows including those of a rotating system. NACA Report No. 1067, 1952.                                               |
| 21         | Cooke, J. C.                                  | A calculation method for three-dimensional turbulent boundary layers. ARC R. and M. No. 3199, October, 1958.                                                                                            |
| 22         | Becker, E.                                    | Berechnung von Reibungsschichten mit schwacher Sekundärströmung nach dem Impulsverfahren. Z. Flugwiss., Vol. 7, p.163, 1959.                                                                            |
| 23         | Zaat, J. A.                                   | Beiträge zur Theorie der dreidimensionalen Grenzschichten. NLL Report MP 190, 1960.                                                                                                                     |

LIST OF REFERENCES (Cont'd)

<u>No.</u>	<u>Author(s)</u>	<u>Title, etc.</u>
24	Braun, W. H.	Turbulent boundary layer on a yawed cone in a supersonic stream. NASA TR R-7. 1959.
25	Spence, D. A.	Velocity and enthalpy distributions in the compressible turbulent boundary layer on a flat plate. J. Fluid Mech. Vol. 8, p.368, 1960.
26	Ludwig, H., Tillmann, W.	Untersuchungen über die Wandschubspannung in turbulenten Reibungsschichten. Ing.-Arch. Vol. 17, p.288, 1949. Translated as NACA TM 1285, 1952, ARC 14800.
27	Spence, D. A.	The growth of compressible turbulent boundary layers on isothermal and adiabatic walls. ARC R. and M. No. 3191, June, 1959.
28	Young, A. D.	The calculation of the profile drag of aerofoils and bodies of revolution at supersonic speeds. Coll. Aeron. Rep. No. 73, ARC 15970, 1953.
29	Thwaites, B. (Ed.)	Incompressible Aerodynamics. Oxford University Press, 1960.
30	Cooke, J. C.	Boundary layers over infinite yawed wings. Aeron. Quart. Vol.11, p.333, 1960.
31	Cooke, J. C.	Turbulent boundary layers over delta wings at zero lift. Unpublished MOA note, 1961.
32	Kehl, A	Über konvergente und divergente turbulente Reibungsschichten. Ing.-Arch., Vol. 13, p.293, 1943.
33	Johnston, J. P.	The turbulent boundary layer at a plane of symmetry in a three-dimensional flow. J of Basic Engineering, Series D, Trans. ASME, Vol.82, p.622, 1960.
34	Moore, R. W. Richardson, D. L.	Skewed boundary-layer flow near the end walls of a compressor cascade. Trans. ASME, Vol.79, p.1789, 1957.
35	Doenhoff, A. E. von Tetervin, N.	Determination of general relations for the behaviour of turbulent boundary layers. NACA Report 772, 1943.
36	Rotta, J.	Näherungsverfahren zur Berechnung turbulenter Grenzschichten unter Benutzung des Energiesatzes. Mitteilungen aus dem Max-Planck-Institut für Strömungsforschung. Nr. 8, Göttingen, 1953.
37	Kopal, Z.	Tables of supersonic flow around yawing cones. M.I.T. Dept. Elec. Eng. Tech. Rep. No.3, 1947.

LIST OF REFERENCES (Cont'd)

<u>No.</u>	<u>Author(s)</u>	<u>Title, etc.</u>
38	Eichelbrenner, E. A. Michel, R.	Observations sur la transition laminaire-turbulent en trois dimensions. La Recherche Aéronautique, No.65, p.3, 1958.
39	Cooke, J. C.	Boundary layer flow between the attachment lines on a flat plate delta wing at incidence. Aero. Quart., Vol. 13, p.1, 1962.
40	Görtler, H.	Über eine dreidimensionale Instabilität laminarer Grenzschichten an konkaven Wänden. ZAMM, Vol. 21, p.250, 1941.
41	Gregory, N.	Transition and the spread of turbulence on a 60° swept-back wing. J. Roy. Aeron. Soc. Vol. 64, p.562, 1960.
42	Gregory, N.	Experiments on transition and on the spread of a turbulence wedge on a 60° swept-back wing. J. Roy. Aeron. Soc. Vol. 64, p.562, 1960.
43	Rotta, J. C.	Turbulent boundary layers in incompressible flow. Chapter in "Progress in Aeronautical Sciences" Vol. 2. Pergamon Press, 1962.
44	Schubauer, G. B., Klebanoff, P. S.	Contributions on the mechanics of boundary-layer transition. NACA Report No. 1289, 1956.

---

ATTACHED:

Appendix 1

---



## APPENDIX 1

### TRANSITION

We shall consider two-dimensional transition as an introduction to the method to be used in the more general case, and will give a "proof" of the continuity of  $\theta$  from elementary considerations. Such a proof cannot be rigorous but it is suggestive.

We assume that the same momentum equation holds on either side of transition. This equation in steady incompressible flow is

$$\frac{d\theta}{dx} + (H + 2) \frac{\theta}{U_e} \frac{dU_e}{dx} = \frac{\tau_w}{\rho U_e^2}, \quad (A1)$$

where  $H = \delta^*/\theta$ .  $\tau_w$  is the wall skin friction and  $U_e$  the external velocity. In turbulent flow there is an additional term

$$\frac{d}{dx} \int_0^{\infty} \frac{\bar{u}'^2 - \bar{v}'^2}{U_e^2} dy,$$

which we shall ignore as is usually done. Thus the same equation applies throughout.

For small  $dx$  equation (A1) may be written, if there are no discontinuities, by the mean value theorem

$$\theta' - \theta + \left[ \frac{(H + 2) \theta}{U_e} \right]_m (U_e' - U_e) = \left[ \frac{\tau_w}{\rho U_e^2} \right]_m dx,$$

where  $[z]_m$  denotes a "mean" value, that is the value  $z$  takes for some value of  $x$  in the range considered, which is taken to include the transition point. Primes denote values at the end of the interval  $dx$ .

We now let  $dx$  tend to zero;  $U_e' \rightarrow U_e$  and although  $H$  and  $\tau_w$  may change rapidly or even be discontinuous in the limit their "mean" values are finite and so

$$\theta = \theta'$$

that is,  $\theta$  is continuous at transition. The result is simply any analytical expression of the fact that there must not be an infinitely large skin friction at transition.

In three dimensions we use equations (9) and (10). If  $\tau_{01}$  and  $\tau_{02}$  are not to be infinite we find that  $\theta_{11}$  and  $\theta_{21}$  must be continuous at transition.

We have arrived at this result on the implicit assumption that the transition front is at right angles to the direction of flow of the external streamlines. If, however, the normal to the front makes an angle  $\alpha'$  with the direction of  $\xi$  increasing the result must be modified. We change the co-ordinate system to  $\xi'$  and  $\eta'$  with  $\xi'$  in the direction normal to the transition front. We now use equations (13) and (14) of Ref.3. They are more complicated but they still lead to the conclusion that  $\theta'_{11}$  and  $\theta'_{21}$  are continuous; here primes denote values in the new co-ordinate system, that is

$$\theta'_{11} = \frac{1}{\rho_e U_e^2} \int_0^\delta (u_e' - u') \rho u' d\xi, \quad \theta'_{21} = \frac{1}{\rho_e U_e^2} \int_0^\delta (v_e' - v') \rho u' d\xi,$$

where  $U_e (= u_e)$  is the resultant external velocity.

Now we have

$$u' = u \cos \alpha' - v \sin \alpha', \quad u_e' = U_e \cos \alpha',$$

$$U' = u \sin \alpha' + v \cos \alpha', \quad v_e' = U_e \sin \alpha',$$

from which we may deduce

$$\theta'_{11} = \cos^2 \alpha' \theta_{11} - \sin \alpha' \cos \alpha' (\theta_{12} + \theta_{21}) + \sin^2 \alpha' \theta_{22}$$

$$\theta'_{21} = \sin \alpha' \cos \alpha' \theta_{11} - \sin^2 \alpha' \theta_{12} + \cos^2 \alpha' \theta_{21} - \sin \alpha' \cos \alpha' \theta_{22},$$

and it is these which must be continuous at transition. They reduce to the previous values when  $\alpha' = 0$  as they should. A neater way of writing the result is found by multiplying these equations respectively by  $\cos \alpha'$  and  $\sin \alpha'$  and adding, and by  $\sin \alpha'$  and  $\cos \alpha'$  and subtracting. We find that

$$\theta_{11} \cos \alpha' - \theta_{12} \sin \alpha' \quad \text{and} \quad \theta_{22} \sin \alpha' - \theta_{21} \cos \alpha'$$

must be continuous at transition.

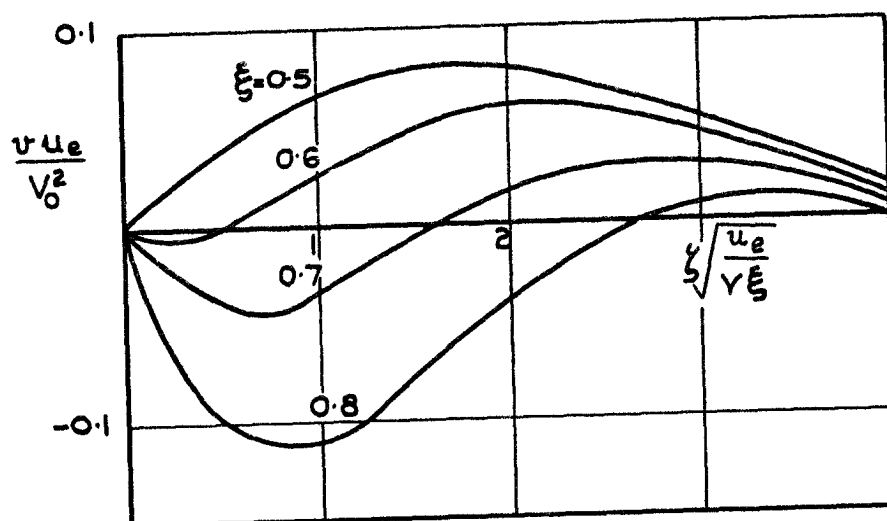


FIG. I. LAMINAR CROSS-FLOW VELOCITY PROFILES. EXTERNAL POINT OF INFLEXION AT  $\xi = 0.5$ .

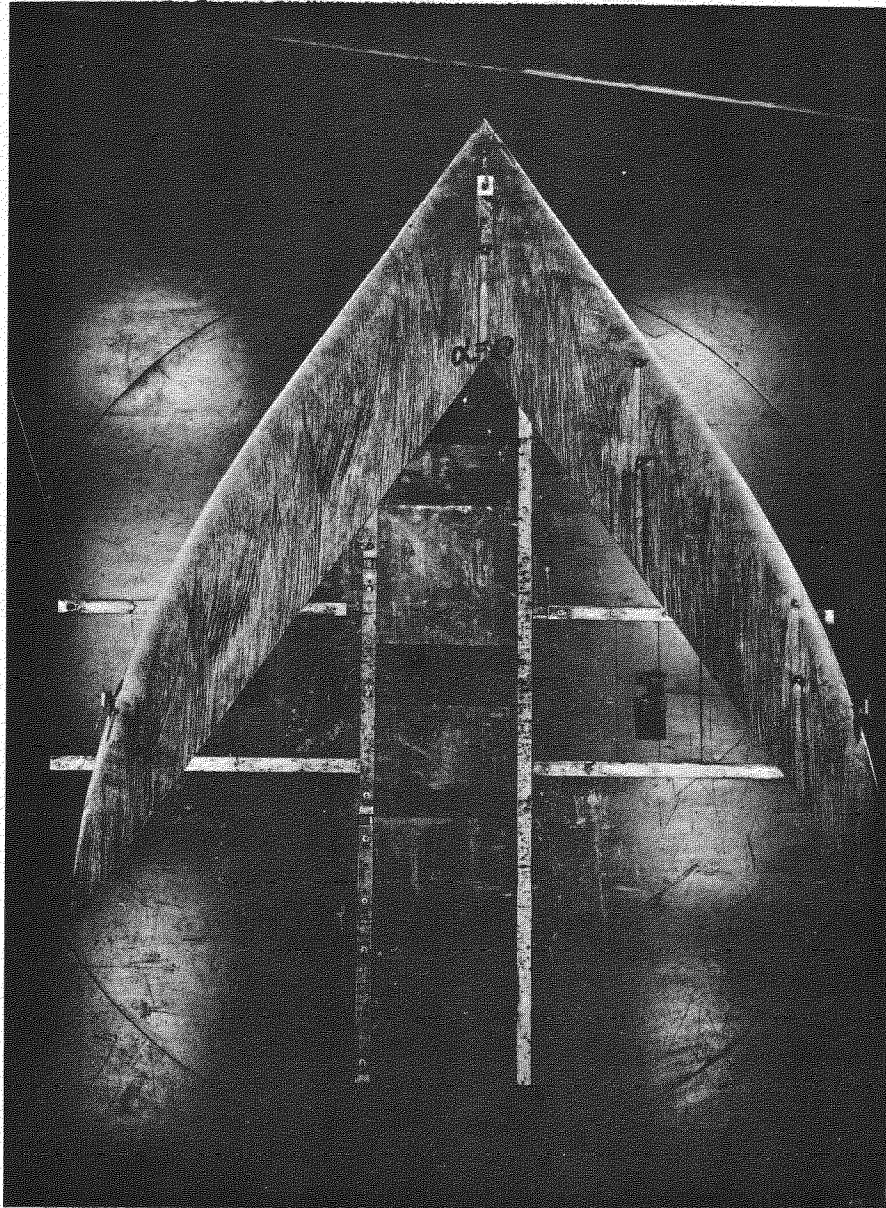


FIG.2. OIL FLOW PATTERNS SHOWING WEDGES OF TURBULENCE. (BREBNER AND WYATT)

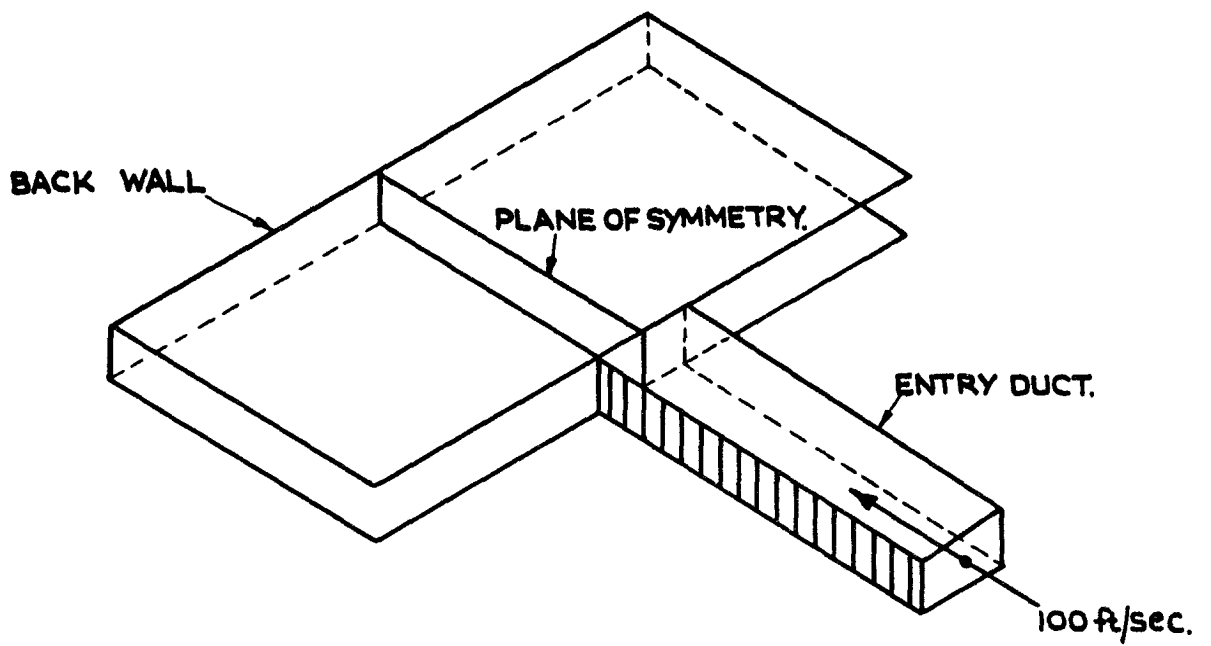


FIG.3. EXPERIMENTAL ARRANGEMENT OF JOHNSTON.

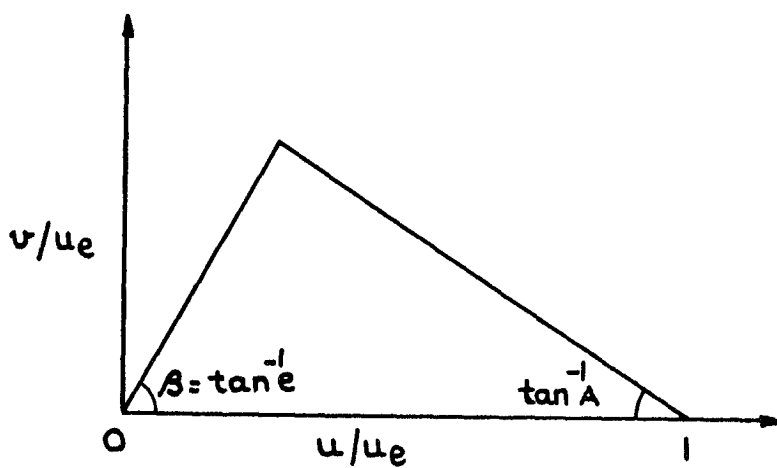


FIG.4. JOHNSTON'S FORM FOR THE CROSS-FLOW.

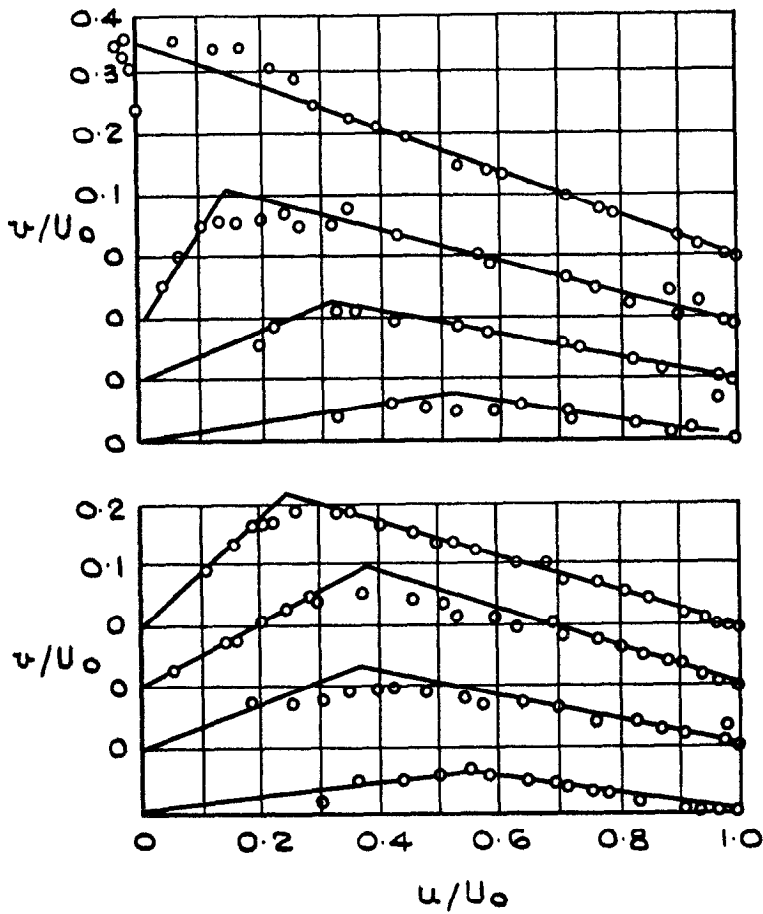


FIG. 5. POLAR PLOTS BY JOHNSTON FROM DATA OF KUETHE ET AL.

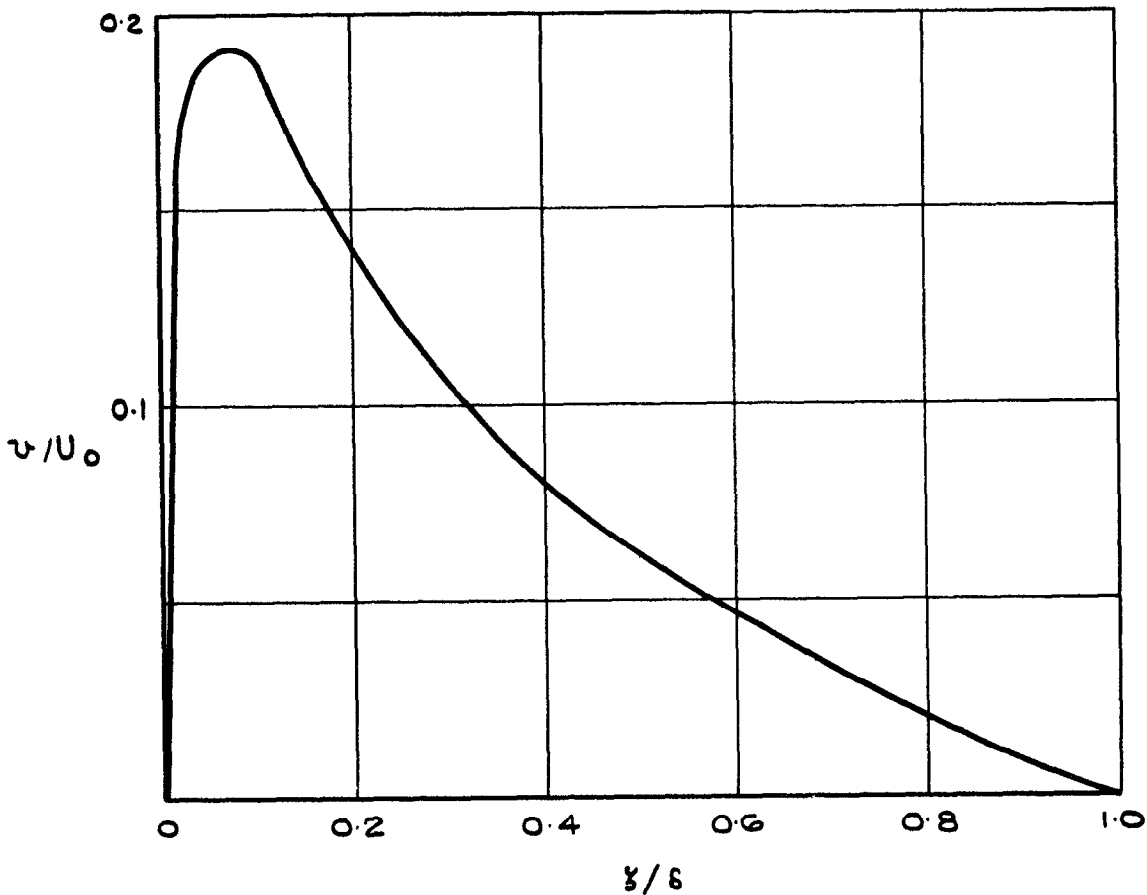


FIG. 6. CROSS-FLOW ACCORDING TO JOHNSTON'S MODEL WITH  $u/u_e = (\gamma/\delta)^{\frac{1}{7}}$ ,  $e = 0.26$ ,  $A = 1.47$ .

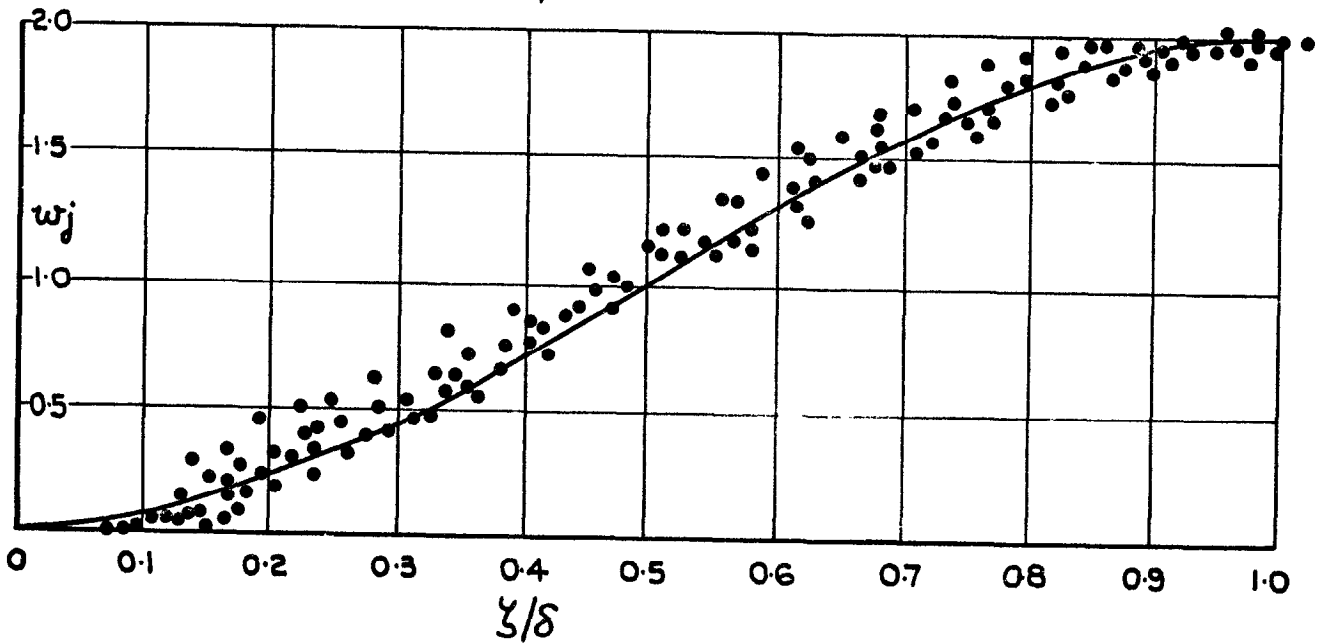
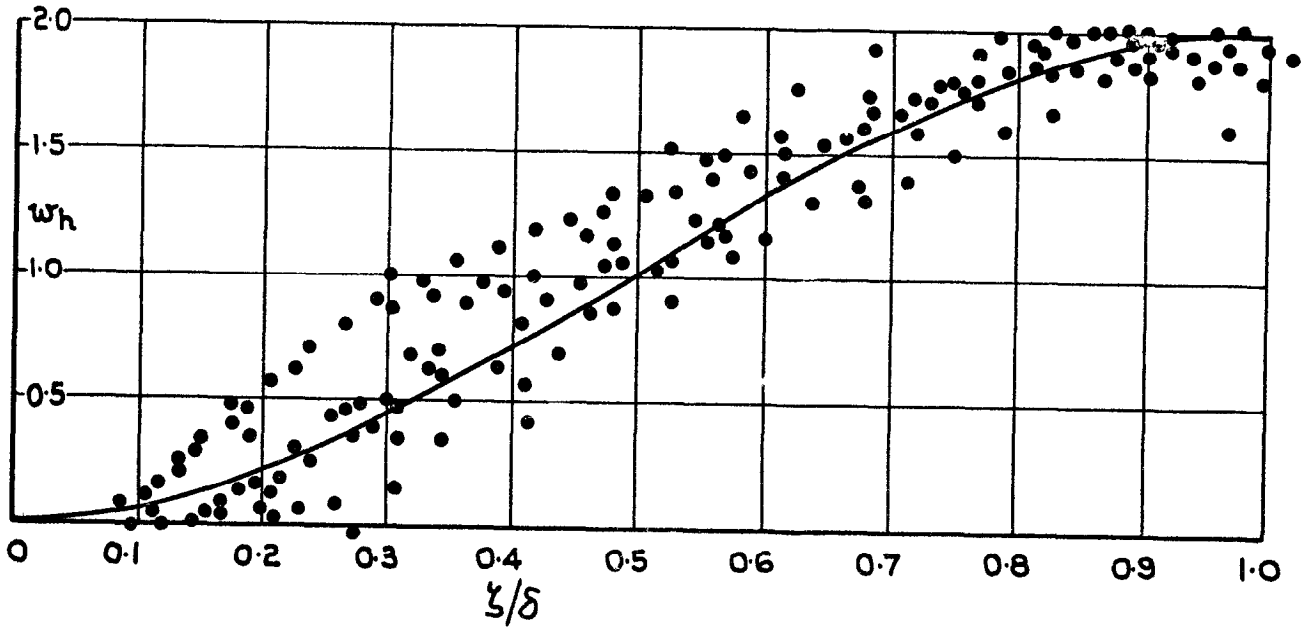


FIG.8. WAKE COMPONENTS  $w_h$  AND  $w_j$   
(BLACKMAN AND JOUBERT)

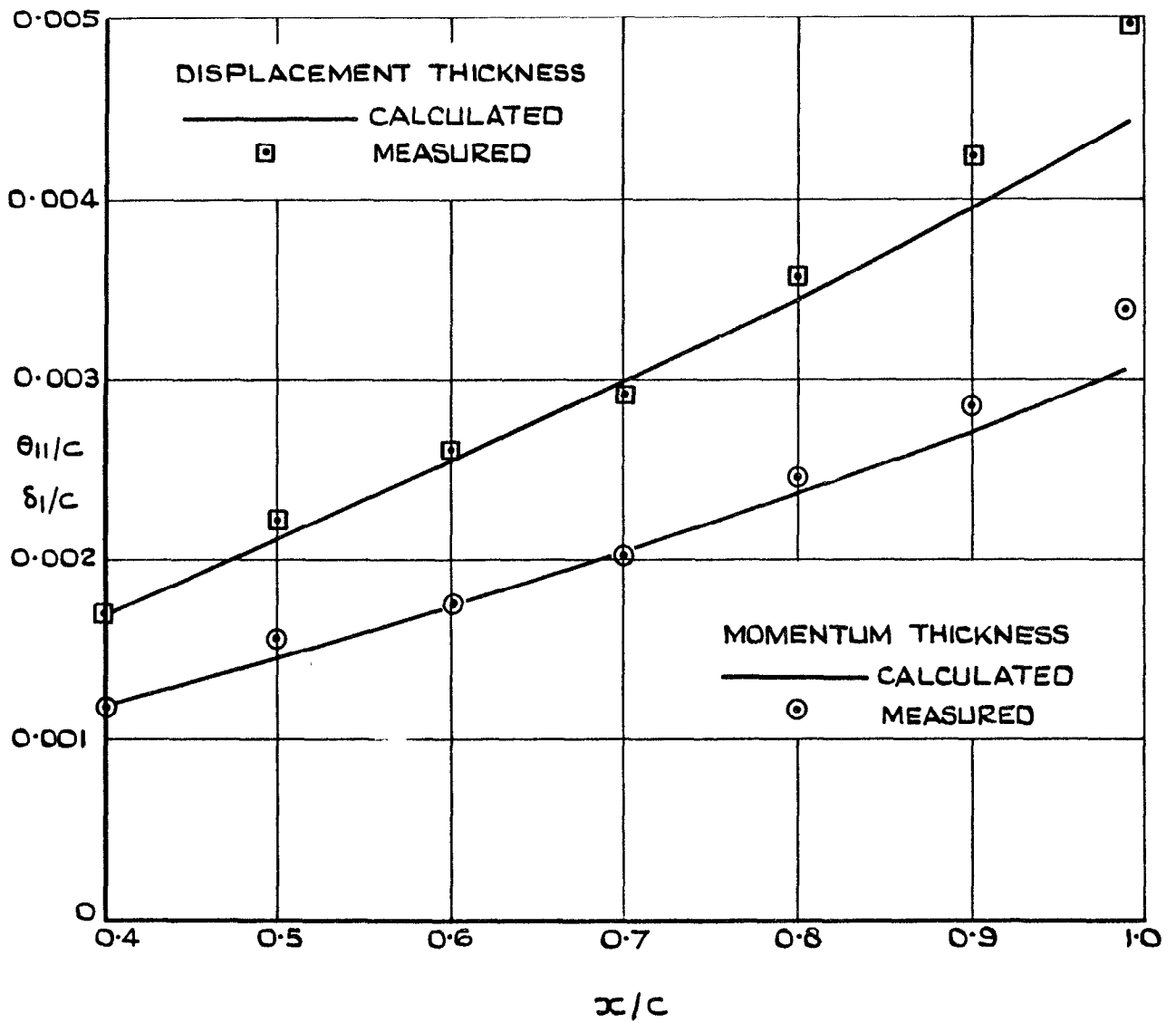


FIG. 9. VALUES OF  $\theta_{11}$  AND  $\delta_1$  FROM MEASUREMENTS BY BREBNER & WYATT



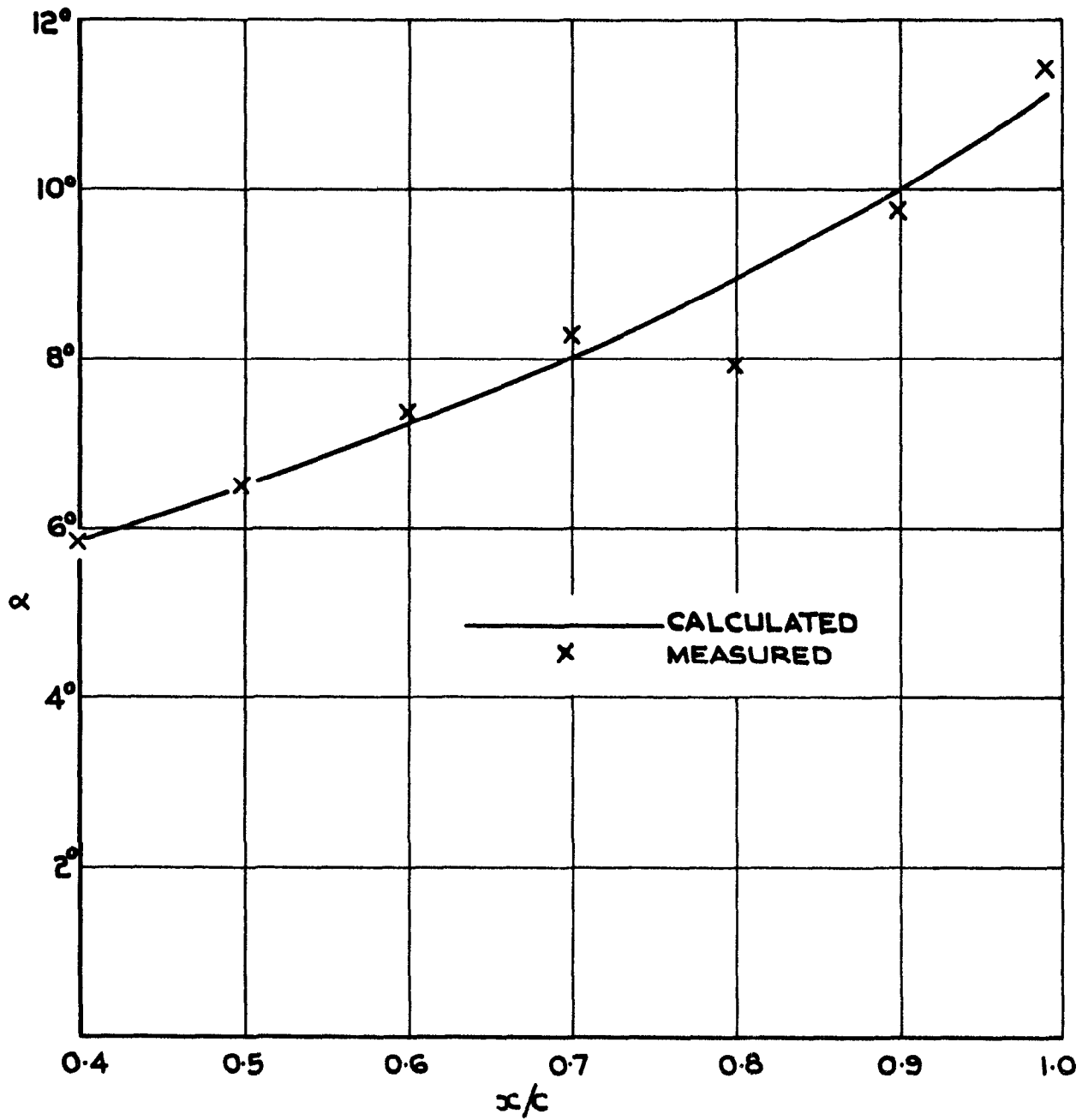


FIG.10. VALUES OF  $\alpha$  FROM MEASUREMENTS BY BREBNER AND WYATT.



FIG.II. CALCULATED EXTERNAL STREAMLINES ON DELTA WING AT ZERO INCIDENCE (COOKE)

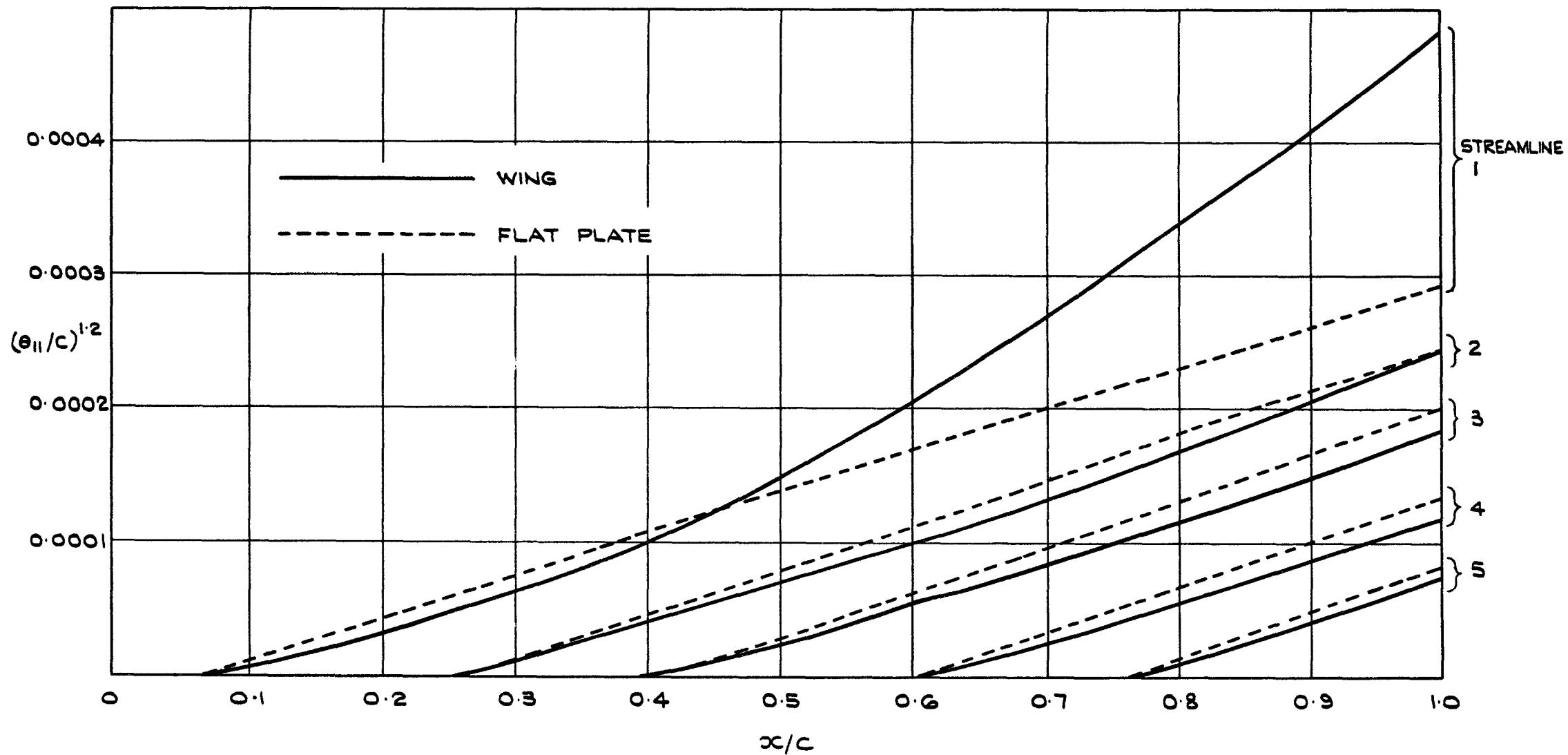


FIG. 12. GROWTH OF MOMENTUM THICKNESS ALONG STREAMLINES OF FIG. II. (COOKE)

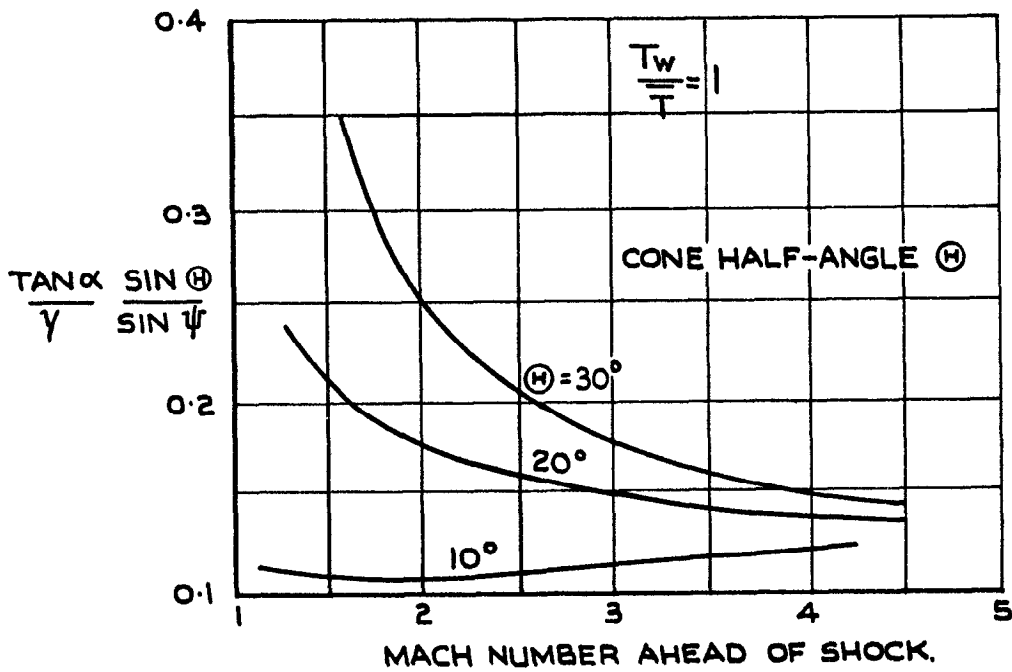
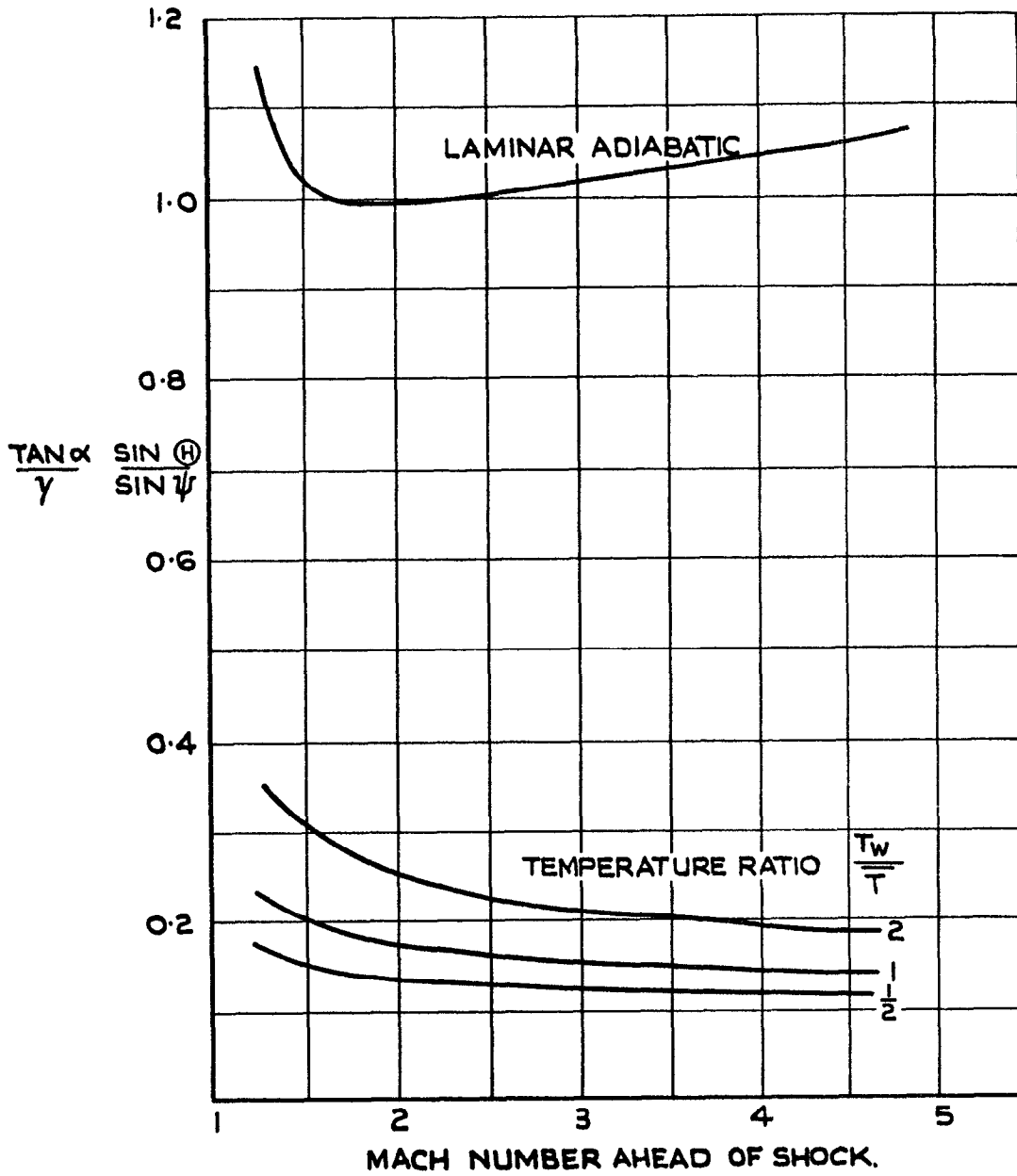


FIG. 13. DEFLECTION OF LIMITING STREAMLINES ON YAWED CONE (BRAUN)

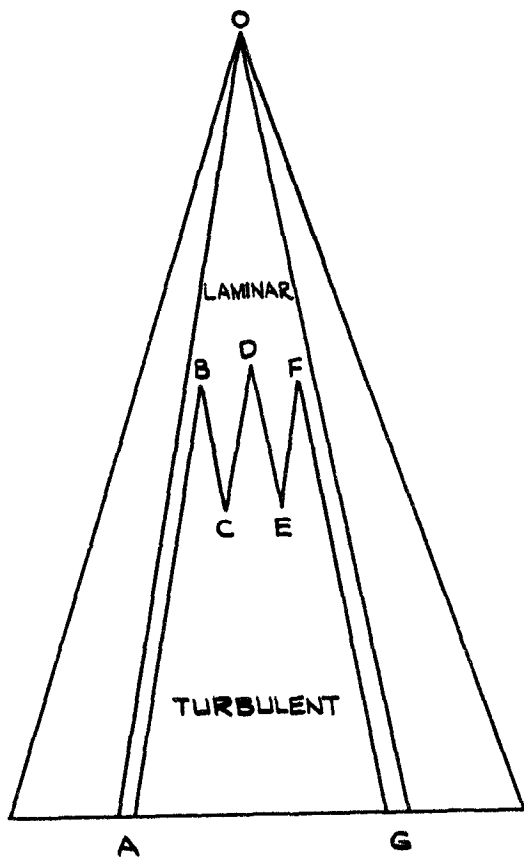


FIG.14. POSSIBLE TRANSITION FRONT (COOKE)

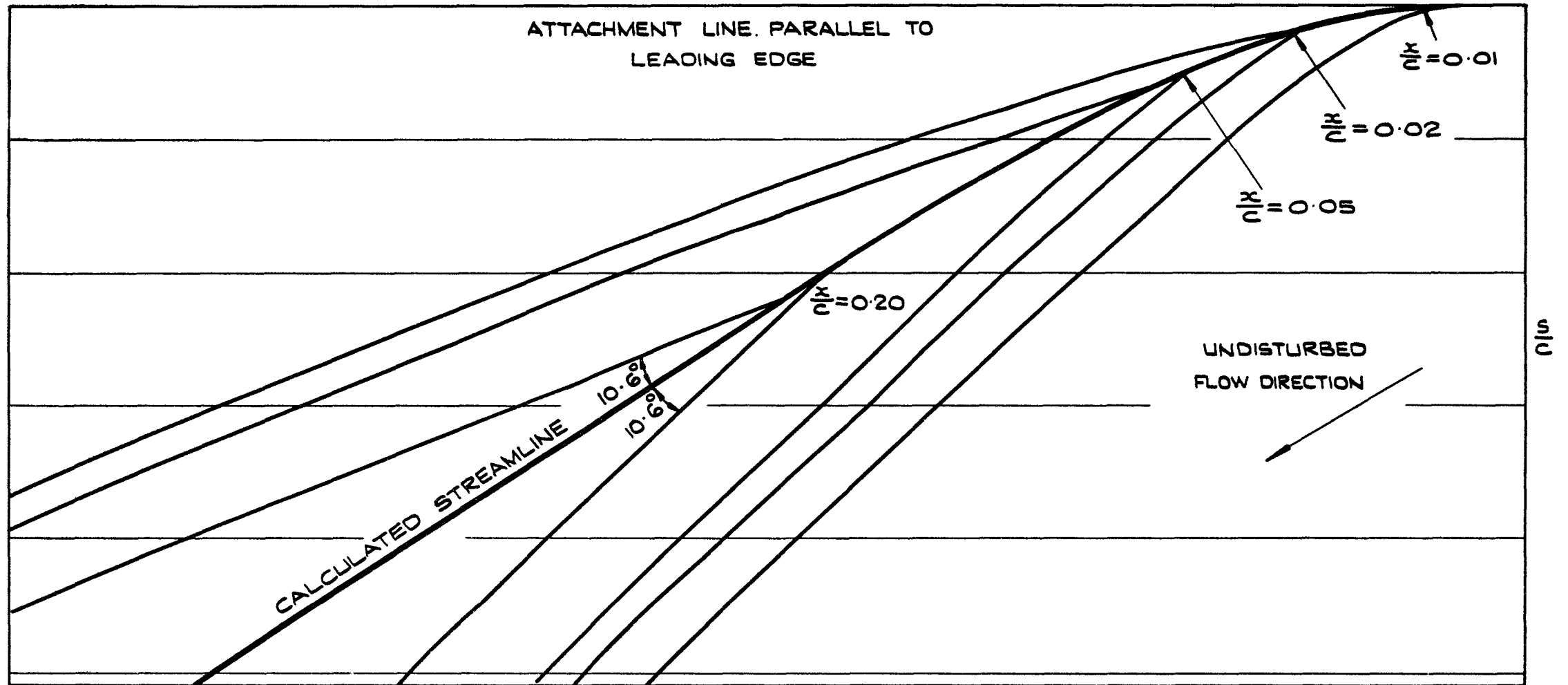


FIG. 15. DEVELOPMENT OF UPPER SURFACE SHOWING CALCULATED STREAMLINE AT  $-3^\circ$  INCIDENCE AND CALCULATED SHAPES OF TURBULENT WEDGES ORIGINATING FROM  $X/C = 0.20, 0.05, 0.02$  AND  $0.01$  POSITIONS (GREGORY.)

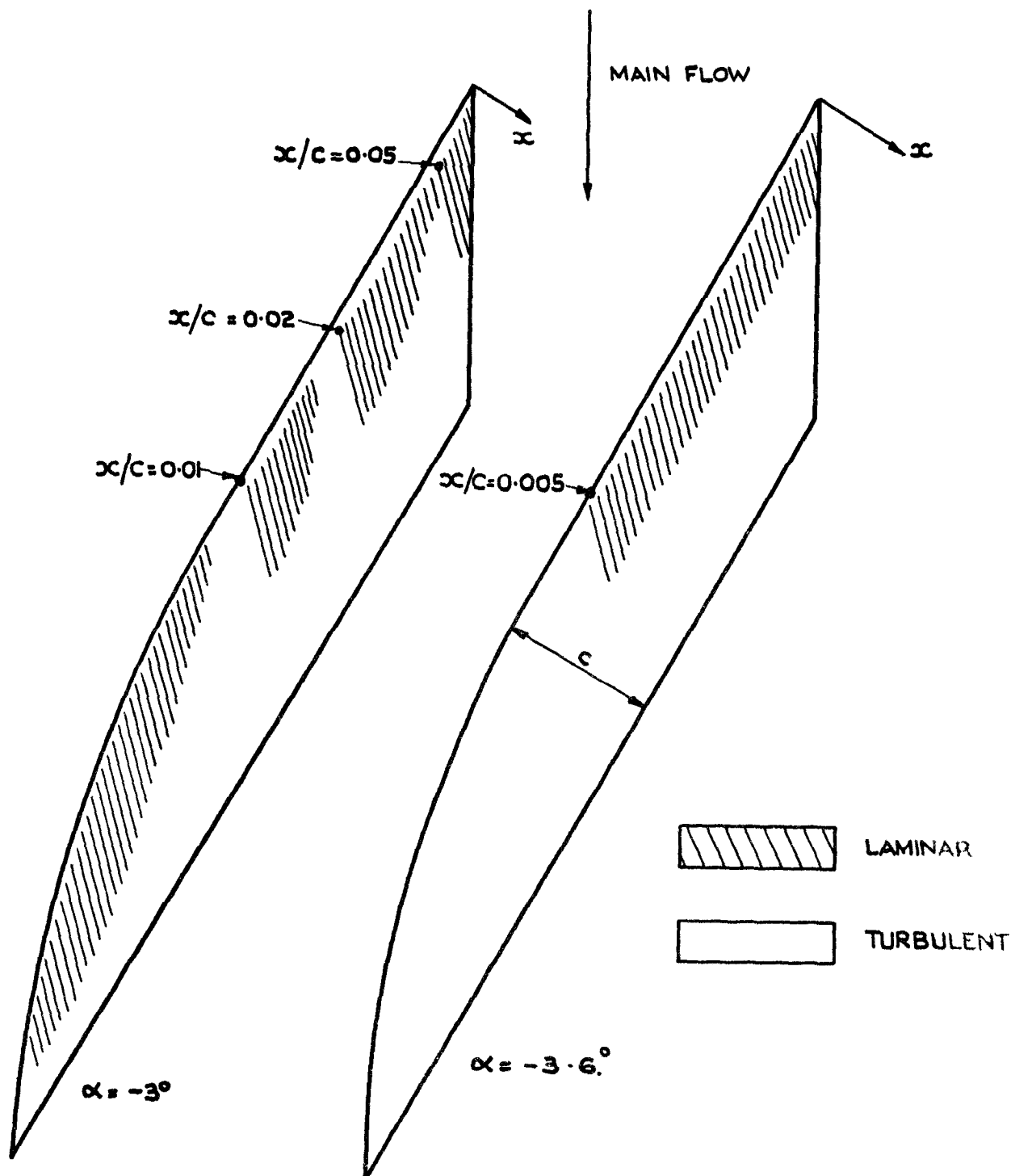


FIG.16. SPREAD OF TURBULENCE DUE TO CONICAL EXCRESCENCES ON  $60^\circ$  SWEEP WING. FROM PHOTOGRAPHS BY GREGORY.

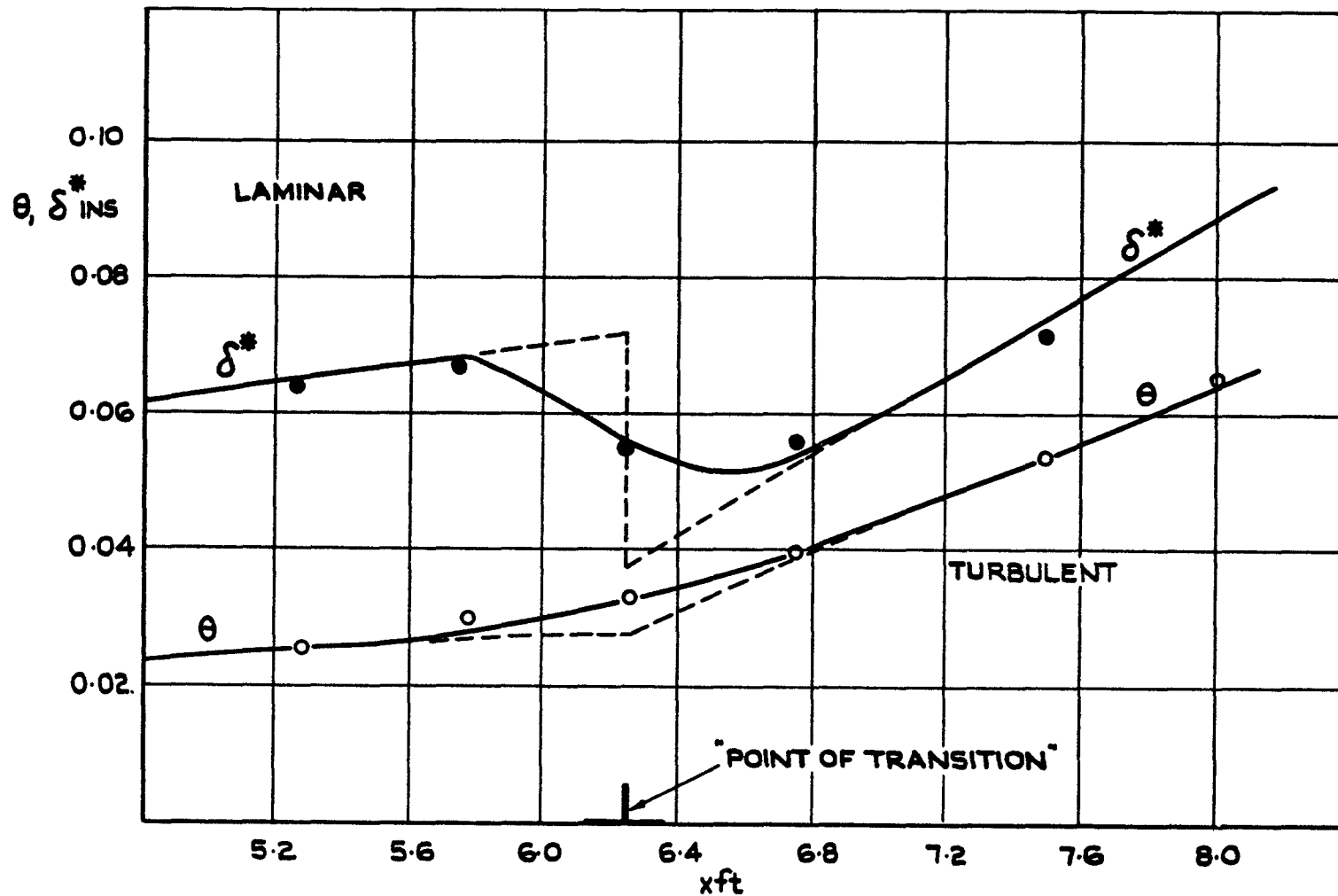


FIG.17. MOMENTUM AND DISPLACEMENT THICKNESS AT TRANSITION. FROM CURVES DRAWN BY ROTTA FROM MEASUREMENTS ON A FLAT PLATE BY SCHUBAUER AND KLEBANOFF.

A.R.C. C.F. No. 635

532.526.4 :  
532.517.4 :  
532.517.3

THREE-DIMENSIONAL TURBULENT BOUNDARY LAYERS  
Cooke, J. C. June, 1961.

This paper reviews the current state of knowledge of three-dimensional turbulent boundary layers, mainly from the point of view of making calculations. The nature of the boundary layer is discussed and the equations for general steady turbulent flow are given. Next follow momentum-integral equations, which can then be solved with suitable assumptions as to the velocity profiles and shear stress components. An account of these assumptions follows and a few sample results are given. The paper ends with a short account of some matters connected with transition.

A.R.C. C.F. No. 635

532.526.4 :  
532.517.4 :  
532.517.3

THREE-DIMENSIONAL TURBULENT BOUNDARY LAYERS  
Cooke, J. C. June, 1961.

This paper reviews the current state of knowledge of three-dimensional turbulent boundary layers, mainly from the point of view of making calculations. The nature of the boundary layer is discussed and the equations for general steady turbulent flow are given. Next follow momentum-integral equations, which can then be solved with suitable assumptions as to the velocity profiles and shear stress components. An account of these assumptions follows and a few sample results are given. The paper ends with a short account of some matters connected with transition.



© *Crown Copyright 1963*

Published by  
**HER MAJESTY'S STATIONERY OFFICE**

To be purchased from  
York House, Kingsway, London W.C.2  
423 Oxford Street, London W.1  
13A Castle Street, Edinburgh 2  
109 St. Mary Street, Cardiff  
39 King Street, Manchester 2  
50 Fairfax Street, Bristol 1  
35 Smallbrook, Ringway, Birmingham 5  
80 Chichester Street, Belfast 1  
or through any bookseller

*Printed in England*